



CERN-EP-2020-92
19 May 2020

First measurement of quarkonium polarization in nuclear collisions at the LHC

ALICE Collaboration*

Abstract

The polarization of inclusive J/ψ and $\Upsilon(1S)$ produced in Pb–Pb collisions at $\sqrt{s_{NN}} = 5.02$ TeV at the LHC is measured with the ALICE detector. The study is carried out by reconstructing the quarkonium through its decay to muon pairs in the rapidity region $2.5 < y < 4$ and measuring the polar and azimuthal angular distributions of the muons. The polarization parameters λ_θ , λ_ϕ and $\lambda_{\theta\phi}$ are measured in the helicity and Collins-Soper reference frames, in the transverse momentum interval $2 < p_T < 10$ GeV/ c and $p_T < 15$ GeV/ c for the J/ψ and $\Upsilon(1S)$, respectively. The polarization parameters for the J/ψ are found to be compatible with zero, within a maximum of about two standard deviations at low p_T , for both reference frames and over the whole p_T range. The values are compared with the corresponding results obtained for pp collisions at $\sqrt{s} = 7$ and 8 TeV in a similar kinematic region by the ALICE and LHCb experiments. Although with much larger uncertainties, the polarization parameters for $\Upsilon(1S)$ production in Pb–Pb collisions are also consistent with zero.

arXiv:2005.11128v2 [nucl-ex] 18 May 2021

1 Introduction

Quarkonia, bound states of charm (c) and anticharm (\bar{c}) or bottom (b) and antibottom (\bar{b}) quarks, represent an important tool to test our understanding of quantum chromodynamics (QCD), since their production process involves both perturbative and non-perturbative aspects. At high energy, the creation of the heavy quark-antiquark pair is a process that can be described using a perturbative QCD approach, due to the large value of the charm and bottom quark masses ($m_c \sim 1.3 \text{ GeV}/c^2$, $m_b \sim 4.2 \text{ GeV}/c^2$ [1]). However, the subsequent formation of the bound state is a non-perturbative process that can be described only by empirical models or effective field theory approaches. Among those, models based on Non-Relativistic QCD (NRQCD) [2] give the most successful description of the production cross section, as measured at high-energy hadron colliders (Tevatron, RHIC, LHC) [3–14]. In the NRQCD approach, the non-perturbative aspects are parameterized via long-distance matrix elements (LDME), corresponding to the possible intermediate color, spin and angular momentum states of the evolving quark-antiquark pair. The values of LDMEs need to be fitted on a subset of the available measurements and can be then considered as universal quantities, in the sense that they can be used in the calculation of production cross sections and other observables corresponding, for example, to different collision systems and energies. Other theory approaches, as the Color Singlet Model [15], the Color Evaporation Model [16] and the k_T -factorization [17] are also used to describe the quarkonium production process.

Among the various charmonium states, the J/ψ meson, with quantum numbers $J^{PC} = 1^{--}$, was the first to be discovered. It is surely the most studied, also due to the sizeable decay branching ratio to dilepton pairs ($(5.961 \pm 0.033)\%$ for the $\mu^+\mu^-$ channel [1]) that represents an excellent experimental signature. While the J/ψ production cross sections are well reproduced by NRQCD-based models, it was soon realized that describing the measured polarization of this state represents a much more difficult problem [18]. The polarization, corresponding to the orientation of the particle spin with respect to a chosen axis, can be accessed via a study of the polar (θ) and azimuthal (ϕ) production angles, relative to that axis, of the two-body decay products in the quarkonium rest frame. Their angular distribution $W(\theta, \phi)$ is parameterized as

$$W(\theta, \phi) \propto \frac{1}{3 + \lambda_\theta} (1 + \lambda_\theta \cos^2 \theta + \lambda_\phi \sin^2 \theta \cos 2\phi + \lambda_{\theta\phi} \sin 2\theta \cos \phi), \quad (1)$$

with the polarization parameters λ_θ , λ_ϕ and $\lambda_{\theta\phi}$ corresponding to various combinations of the elements of the spin density matrix of J/ψ production [19]. In particular, the two cases ($\lambda_\theta = 1$, $\lambda_\phi = 0$, $\lambda_{\theta\phi} = 0$) and ($\lambda_\theta = -1$, $\lambda_\phi = 0$, $\lambda_{\theta\phi} = 0$) correspond to the so-called transverse and longitudinal polarizations, respectively. At leading order, the high- p_T production is dominated by gluon fragmentation and therefore the J/ψ would be expected to be transversely polarized [18]. However, the results from the CDF experiment at Tevatron showed that the J/ψ exhibits a very small polarization [20, 21], an observation which was impossible to reconcile with the NRQCD prediction. As of today, on the experimental side, accurate results on inclusive and prompt (i.e., removing contributions from b-quark decays) J/ψ polarization have become available at LHC energies [22–25]. They confirm that this state shows little or no polarization in a wide rapidity (up to $y = 4.5$) and transverse momentum region (from 2 to 70 GeV/c), with the exception of the LHCb measurements at $\sqrt{s} = 7 \text{ TeV}$ [24], where the value $\lambda_\theta = -0.145 \pm 0.027$, corresponding to a weak longitudinal polarization, was obtained in the interval $2 < p_T < 15 \text{ GeV}/c$ and $2 < y < 4.5$, in the helicity frame (its definition will be given later in Sec. 3). On the theory side, a huge effort was pursued in order to move to a complete next-to-leading order (NLO) description of the J/ψ production process [26, 27], and to the calculation of the polarization variables [28, 29]. Further important progress includes a quantitative evaluation of the contribution of feed-down processes (J/ψ coming from the decay of χ_c and $\psi(2S)$ states) on the polarization observables [30]. It was shown that at NLO there are rather large cancellations between contributions corresponding to the different possible combinations of

the spin and angular momentum of the intermediate $c\bar{c}$ states, reaching a more satisfactory description of the absence of polarization observed in the data [31]. However, those descriptions usually require the inclusion of both cross section and polarization results in the fit of the LDME, leading to a more limited predictive power on the polarization observables and to large variations in the values of the extracted LDME values, depending on the set of data used for their determination. Finally, the description of the J/ψ production in the NRQCD framework was recently extended to the low- p_T region, and the polarization parameters were studied in a color glass condensate (CGC) + NRQCD formalism, obtaining a fair agreement with LHC data at forward rapidity [32]. Measurements of the polarization parameters are also available for several bottomonium states, and in particular for the $\Upsilon(1S)$, $\Upsilon(2S)$ and $\Upsilon(3S)$ resonances, which were shown to exhibit little or no polarization at LHC energies [33–35]. Approaches similar to that adopted for charmonium, which also need to take into account the rather complex feed-down decay structure for these states, lead to a fair agreement with the experimental results [36].

In this Letter, we move a step forward by presenting the first measurement of J/ψ and $\Upsilon(1S)$ polarization in ultrarelativistic heavy-ion interactions performed by the ALICE Collaboration by studying Pb–Pb collisions at $\sqrt{s_{NN}} = 5.02$ TeV. Such collisions represent an important source of information for the investigation of the phase diagram of QCD [37], and in particular for the study of the properties of the quark–gluon plasma (QGP), a state of matter where quarks and gluons are not confined inside hadrons [38]. Among the experimental observables studied in heavy-ion collisions the suppression of heavy quarkonium production is a fundamental signal, since QGP formation prevents the binding of the heavy-quark pair due to the screening of the color charge [39] and, more generally, has strong effects on the spectral functions [40]. At LHC energies, another mechanism, corresponding to the (re)generation of charmonium states in the QGP and/or when the system hadronizes, becomes relevant [41, 42], in particular at low p_T , due to the large charm-quark multiplicity (> 100 pairs in a central Pb–Pb collision). The presence of a deconfined system may in principle affect also the polarization of quarkonium states. In Ref. [43] the observation of a partial transverse polarization for the J/ψ was predicted in case of QGP formation, due to a modification of the non-perturbative effects in the high energy-density phase. More generally, the observed prompt J/ψ are known to be a mixture of direct production and decay products from higher-mass charmonium states ($\psi(2S)$, χ_c). In nuclear collisions, since suppression effects are expected to affect more strongly the less bound states, the relative contribution of direct and feed-down production would change with respect to that in pp collisions, and the overall measured polarization may be different according to the potentially different polarization of the various states [44, 45]. On the other hand, the contribution of the regeneration mechanism in the J/ψ formation process by recombination of uncorrelated $c\bar{c}$ pairs is likely to give rise to unpolarized production at low p_T . Finally, the possible presence of polarization is known to strongly affect the acceptance for J/ψ detection in the dilepton decay (up to 20–30% in ALICE [22]), and its measurement is an important requisite for an unbiased evaluation of the absolute yields in nuclear collisions. A first measurement of $\Upsilon(1S)$ polarization in Pb–Pb collisions is also presented in this Letter, even if the corresponding candidate sample is smaller by a factor ~ 30 , leading to larger uncertainties. For such a state, considerations similar to those discussed for the J/ψ should hold, except that the contribution of the regeneration mechanism should be negligible due to the much lower multiplicity of bottom quarks with respect to charm.

The next sections of the Letter are organized as follows. Section 2 contains a short description of the experimental apparatus and some details on the data sample used in this analysis. The analysis procedure and the evaluation of systematic uncertainties are presented in Sec. 3, while the results on the J/ψ and $\Upsilon(1S)$ polarization parameters λ_θ , λ_ϕ and $\lambda_{\theta\phi}$ are shown in Sec. 4. The conclusions are presented in Sec. 5.

2 Experimental setup and data sample

The measurement described in this Letter is performed with the ALICE detector [46, 47], whose main components are a central barrel and a forward muon spectrometer. The latter covers the pseudorapidity region $-4 < \eta < -2.5$ and is used to detect muon pairs from quarkonium decays [48]. The muon spectrometer includes a hadron absorber made of concrete, carbon and steel with a thickness of 10 interaction lengths, followed by five tracking stations (cathode-pad chambers), with the central one embedded inside a dipole magnet with a 3 T·m field integral. Downstream of the tracking system, an iron wall filters out the remaining hadrons as well as low-momentum muons originating from pion and kaon decays, and is followed by two trigger stations (resistive plate chambers). Another forward detector, the V0 [49], composed of two scintillator arrays located at opposite sides of the interaction point (IP) and covering the pseudorapidity intervals $-3.7 < \eta < -1.7$ and $2.8 < \eta < 5.1$, provides the minimum bias (MB) trigger which is given by a coincidence of signals from the two sides. Among the central barrel detectors, the two layers of the Silicon Pixel Detector (SPD), with $|\eta| < 2$ and $|\eta| < 1.4$ coverage, and corresponding to the inner part of the ALICE Inner Tracking System (ITS) [50], are used to determine the position of the interaction vertex. Finally, the Zero Degree Calorimeters (ZDC) [51], located on either side of the IP at ± 112.5 m along the beam axis, detect spectator nucleons emitted at zero degrees with respect to the LHC beam axis and are used to reject electromagnetic Pb–Pb interactions.

The analysis is based on events where, in addition to the MB condition, two opposite-sign tracks are detected in the triggering system of the muon spectrometer (dimuon trigger). The dimuon trigger selects tracks each having a transverse momentum above a threshold nominally set at $p_T^\mu = 1$ GeV/ c , corresponding to the value for which the single-muon trigger efficiency reaches 50% [52]. The single-muon trigger efficiency reaches a plateau value of 98% at ~ 2.5 GeV/ c .

The events are further characterized according to their centrality, i.e., the degree of geometric overlap of the colliding nuclei. It is estimated by means of a Glauber model fit to the V0 signal amplitude distribution [53, 54], with more central events leading to a larger signal in the V0. In this analysis, events corresponding to the most central 90% of the inelastic Pb–Pb cross section are selected, as for these events the MB trigger is fully efficient and the residual contamination from electromagnetic processes is negligible.

The results of the analysis are obtained using the $\sqrt{s_{NN}} = 5.02$ TeV Pb–Pb data samples collected by the ALICE experiment during the years 2015 and 2018, corresponding to an integrated luminosity $L_{int} \sim 750 \mu\text{b}^{-1}$.

3 Data analysis

The J/ψ and $\Upsilon(1S)$ candidates are formed by combining opposite-sign muons reconstructed using the tracking algorithm described in Ref. [48]. In order to reject tracks at the edge of the spectrometer acceptance, the condition $-4 < \eta_\mu < -2.5$ is required. In addition, tracks must have a radial transverse position at the end of the absorber in the range $17.6 < R_{abs} < 88.9$ cm. This selection is applied to remove tracks passing through the inner and denser part of the absorber, which are strongly affected by multiple scattering. For each muon candidate, a match between tracks reconstructed in the tracking system and track segments in the muon trigger system is required.

The J/ψ polarization parameters λ_θ , λ_ϕ and $\lambda_{\theta\phi}$ are studied as a function of transverse momentum in the intervals $2 < p_T < 4$, $4 < p_T < 6$ and $6 < p_T < 10$ GeV/ c . For each p_T interval, a two-dimensional (2D) grid of dimuon invariant-mass spectra is created, corresponding to intervals in $\cos \theta$ and ϕ , where θ and ϕ are the polar and azimuthal emission angles, respectively, of the decay products in the J/ψ rest frame, with respect to the reference axis. More in detail, the 2D grid covers the fiducial region $-0.8 < \cos \theta < 0.8$ (17 intervals), $0.5 < \phi < \pi - 0.5$ rad (8 intervals, assuming a symmetric distribution around $\phi = \pi$), with

the choice of the boundaries as well as the width of the intervals dictated by acceptance considerations.

The analysis is performed choosing two different reference systems for the determination of the angular variables. In the Collins-Soper (CS) frame the z -axis is defined as the bisector of the angle between the direction of one beam and the opposite of the direction of the other one in the rest frame of the decaying particle, allowing therefore an evaluation of the polarization parameters with respect to the direction of motion of the colliding hadrons. In the helicity (HE) reference frame the z -axis is given by the direction of the decaying particle in the center-of-mass frame of the collision, and therefore the polarization can be evaluated with respect to the momentum direction of the J/ψ itself. The $\phi = 0$ plane is the one containing the two beams in the J/ψ rest frame.

For each dimuon invariant-mass spectrum, the J/ψ raw yield is obtained by means of a binned maximum likelihood fit in the interval $2.1 < m_{\mu\mu} < 4.9 \text{ GeV}/c^2$. The background continuum is parameterized with a Gaussian distribution whose width varies linearly with the mass or, alternatively, with a fourth degree polynomial function times an exponential. The J/ψ signal is modeled with a pseudo-Gaussian function or with a Crystal Ball function with asymmetric tails on both sides of the peak [55].

The J/ψ mass is kept free in the fits, while for each interval (i,j) in $(\cos\theta, \phi)$ the width is fixed to $\sigma_{J/\psi}^{i,j} = \sigma_{J/\psi}^{i,j,MC} \cdot (\sigma_{J/\psi} / \sigma_{J/\psi}^{MC})$, i.e., scaling the resonance width extracted from Monte Carlo (MC) simulations ($\sigma_{J/\psi}^{i,j,MC}$) by the ratio between the width obtained by fitting the angle-integrated spectrum in data ($\sigma_{J/\psi}$) and MC ($\sigma_{J/\psi}^{MC}$) for the p_T interval under consideration. The parameters of the non-Gaussian tails of the resonance are kept fixed to the MC values. The $\psi(2S)$ contribution, although comparatively negligible, is also taken into account in the fits, with its width and mass fixed in each fit to those of the J/ψ according to the relations $\sigma_{\psi(2S)} = \sigma_{J/\psi} \cdot \sigma_{\psi(2S)}^{MC} / \sigma_{J/\psi}^{MC}$ and $m_{\psi(2S)} = m_{J/\psi} + m_{\psi(2S)}^{PDG} - m_{J/\psi}^{PDG}$, with the Particle Data Group (PDG) masses taken from Ref. [1]. In Fig. 1 (left) an example of a fit to the invariant-mass spectrum in the J/ψ mass region is shown. Due to the stability of the extracted J/ψ parameters (mass, width), the fits were carried out directly on the sum of the 2015 and 2018 invariant mass spectra.

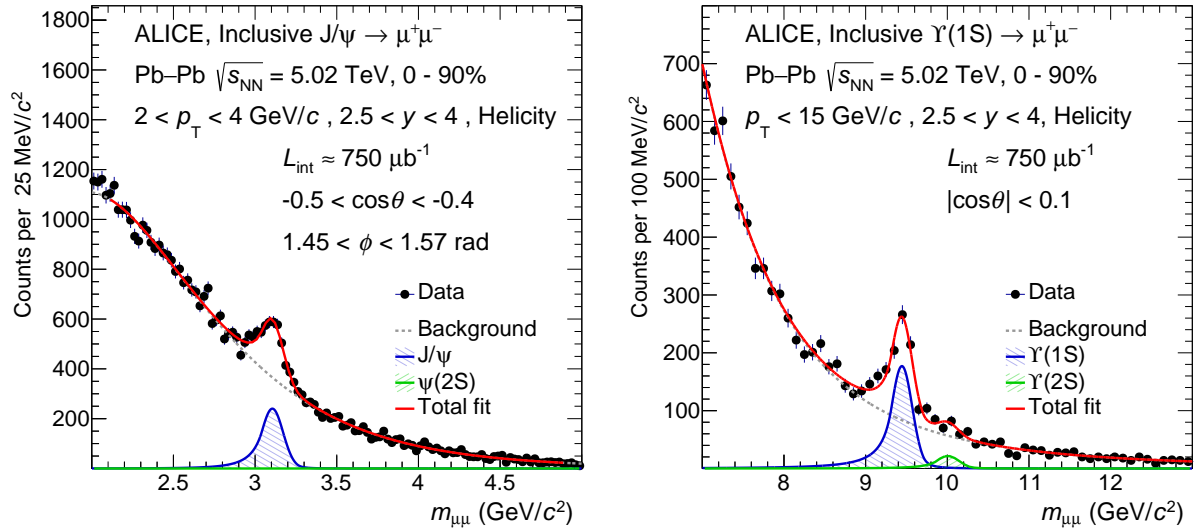


Figure 1: Examples of fits to the invariant-mass distributions in the helicity reference frame. The left plot corresponds to the J/ψ mass region, while on the right a fit to the $\Upsilon(1S)$ mass region is shown. The fits are performed using an extended Crystal Ball function for the resonance signals, while the background is parameterized with a variable width Gaussian.

The J/ψ raw yields as a function of the angular variables are then corrected by the product of the acceptance and detector efficiency ($A \times \epsilon$), which is evaluated as a function of $\cos\theta$ and ϕ on a 2D grid via

MC simulations. The J/ψ are generated according to p_T and y distributions directly tuned on data [56] via an iterative procedure [57], and their decay muons are propagated inside a realistic description of the ALICE setup, based on GEANT 3.21 [58]. The misalignment of the detection elements and the time-dependent status of each electronic channel during the data taking period are taken into account as well. In the J/ψ generation an isotropic distribution of decay products, corresponding to the assumption of no polarization, is adopted. Due to the choice of relatively small ($\cos \theta$, ϕ) intervals, the $A \times \varepsilon$ values for each interval are quite insensitive to the specific angular distribution assumed in the generation.

The three polarization parameters λ_θ , λ_ϕ and $\lambda_{\theta\phi}$ are obtained through χ^2 -minimization fits of the 2D J/ψ distributions, corrected for acceptance and efficiency, according to Eq. 1. For each combination of signal and background shape used in the fit to the dimuon invariant-mass spectra, a separate evaluation of the polarization parameters is carried out and their average is taken as the best estimate. The statistical uncertainty is given by the average of the statistical uncertainties of the 2D fits, while the root mean square of the results provides the systematic uncertainty on the signal extraction, with the absolute values ranging between 0.002 and 0.039. The overall procedure described above was checked beforehand with a MC closure test. The 2D fits on the ($\cos \theta$, ϕ) distributions only allow a determination of the absolute value of $\lambda_{\theta\phi}$, due to the presence of $\sin 2\theta$ in the corresponding term that induces an ambiguity in its sign. It is checked that the values of λ_θ and λ_ϕ are stable against the choice of the sign of the $\lambda_{\theta\phi}$ term. In the following the $\lambda_{\theta\phi}$ values corresponding to the choice of a positive sign are quoted. Figure 2 illustrates an example of the fit to the angular distributions. For better visibility, both the distribution and the fitted function are projected along one dimension.

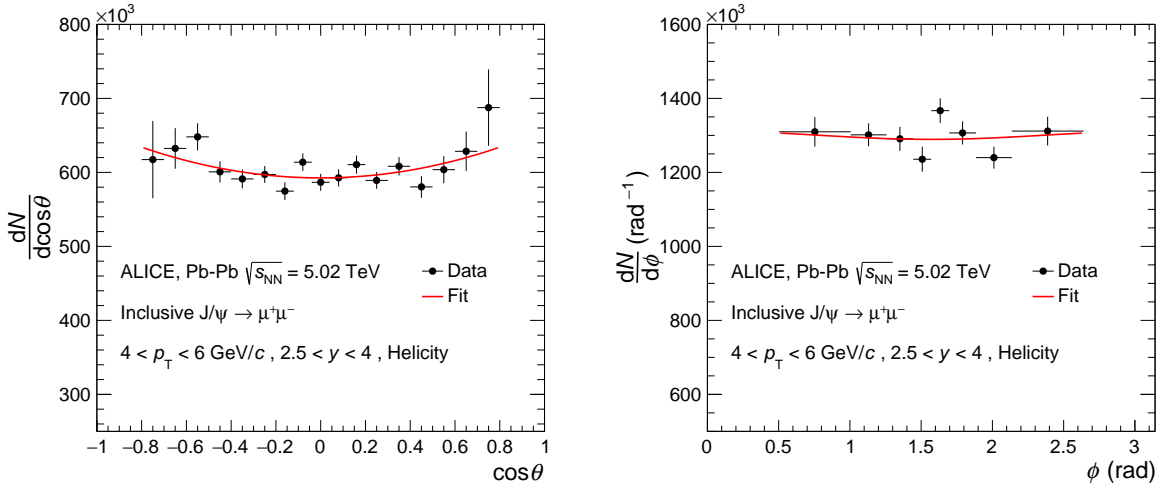


Figure 2: Fit to the J/ψ 2D angular distributions in the helicity reference frame projected along $\cos \theta$ (left) and ϕ (right) for $2.5 < y < 4$ and $4 < p_T < 6$ GeV/c. The displayed uncertainties are statistical.

In addition to the systematic uncertainty related to the choice of the mass shapes for signal and background, several other sources are taken into account. First, an alternative procedure for extracting the J/ψ signal is carried out, by keeping its width as a free parameter in the invariant-mass fits. The corresponding results for the polarization parameters are then obtained and the averages of the values corresponding to fixing the width or not are taken as the central values for λ_θ , λ_ϕ and $\lambda_{\theta\phi}$. Half the difference between the results obtained with free or MC-anchored widths is then considered as a further systematic uncertainty related to the signal extraction. This uncertainty is found to be the leading contribution to the total absolute systematic uncertainty on the polarization parameters, and ranges between 0.001 and 0.063, the latter value corresponding to the uncertainty on $\lambda_\theta^{\text{HE}}$ for $2 < p_T < 4$ GeV/c.

Another source of systematic uncertainty is related to the evaluation of the trigger efficiency. The muon trigger response function as a function of the single muon transverse momentum p_T^μ can be obtained via

MC or with a procedure based on data [59]. Small deviations are found for $p_T^\mu < 2$ GeV/ c which induce an effect on $A \times \varepsilon$ for the J/ψ . Therefore, the polarization parameters are re-calculated with $A \times \varepsilon$ values weighted in such a way to account for the deviations. The variation of the polarization parameters between the different trigger efficiency estimates is taken as the related systematic uncertainty, with values ranging from 0.001 to 0.043, the highest values being found for $\lambda_\theta^{\text{HE}}$ in $2 < p_T < 4$ GeV/ c . The systematic uncertainty related to the evaluation of the muon tracking efficiency is found to be negligible for this analysis, allowing a significant reduction of the total systematic uncertainty with respect to previous pp analyses [23]. Indeed, although the difference between efficiencies calculated via MC or from data [59] is of the order of 2%, a detailed investigation has shown no dependence on the angular variables and therefore no effect on the polarization parameters.

Finally, the systematic uncertainty induced by the choice of the p_T and y distributions used as an input for the calculation of $A \times \varepsilon$ is evaluated testing alternative p_T and y parameterizations, which are obtained by varying within their uncertainties the default distributions directly tuned on Pb–Pb data. The polarization parameters extracted with the modified values of $A \times \varepsilon$ are compared with those obtained with the default input shapes and the corresponding systematic uncertainty extracted in this way is found to range between 0.001 and 0.030, with the largest value assigned to $\lambda_\theta^{\text{HE}}$ for $2 < p_T < 4$ GeV/ c . The influence of the choice of the angular distributions of the J/ψ decay products for the $A \times \varepsilon$ calculation is also investigated by means of an iterative procedure on these input distributions. The effect is found to be negligible, also due to the fact that the 2D correction procedure on the angular variables is by definition relatively insensitive to the specific choice of the corresponding distributions. A summary of the values of all the absolute systematic uncertainties, which are considered as uncorrelated as a function of p_T , is reported in Table 1. The total systematic uncertainties are obtained, for each parameter and p_T interval, as the quadratic sum of the values.

Table 1: Summary of the absolute systematic uncertainties on the evaluation of the J/ψ polarization parameters. All the uncertainties are considered as uncorrelated as a function of p_T .

	p_T (GeV/ c)	Helicity				Collins-Soper			
		Signal extr.	J/ψ width	Trigger eff.	Input MC	Signal extr.	J/ψ width	Trigger eff.	Input MC
λ_θ	$2 < p_T < 4$	0.030	0.063	0.043	0.030	0.026	0.049	0.015	0.009
	$4 < p_T < 6$	0.017	0.046	0.040	0.024	0.002	0.052	0.018	0.007
	$6 < p_T < 10$	0.039	0.005	0.018	0.017	0.022	0.001	0.011	0.006
λ_ϕ	$2 < p_T < 4$	0.007	0.030	0.004	0.002	0.024	0.010	0.020	0.003
	$4 < p_T < 6$	0.003	0.035	0.003	0.003	0.002	0.010	0.020	0.003
	$6 < p_T < 10$	0.002	0.009	0.001	0.002	0.005	0.013	0.011	0.002
$\lambda_{\theta\phi}$	$2 < p_T < 4$	0.021	0.029	0.024	0.001	0.013	0.010	0.017	0.015
	$4 < p_T < 6$	0.007	0.011	0.017	0.006	0.002	0.042	0.010	0.015
	$6 < p_T < 10$	0.020	0.019	0.007	0.008	0.007	0.042	0.003	0.013

A similar procedure is followed for the extraction of the $\Upsilon(1S)$ polarization parameters. Due to the smaller candidate sample, integrated values over the kinematic interval $2.5 < y < 4$, $p_T < 15$ GeV/ c are obtained. The main difference with respect to the 2D approach followed for the J/ψ is the use of a simultaneous fit to the 1D angular distributions [23], after integration over the other variables. The requirement $p_T^\mu > 2$ GeV/ c , which helps reducing the combinatorial background, is included [60]. The $\Upsilon(1S)$ signal extraction in the various $\cos\theta$ and ϕ intervals is performed by means of invariant-mass fits (see the right panel of Fig. 1 for an example). The functions chosen for the resonances are the same as in the J/ψ analysis (pseudo-Gaussian or Crystal Ball), the mass value is fixed to that obtained from a fit to the integrated invariant-mass distribution, while the width for each angular interval is fixed to the

MC value scaled by the ratio of the widths between data and MC for the angle-integrated distributions. The tail parameters are fixed to MC values. The small contribution from $\Upsilon(2S)$ is also included in the fits [60]. The background continuum is parameterized with a Gaussian distribution whose width varies linearly with the mass or, alternatively, with a second degree polynomial function times an exponential. The systematic uncertainty on the signal extraction is calculated with the same procedure adopted for the J/ψ . An uncertainty related to the choice of the signal width has also been considered, taken as the half-difference between the results obtained with the prescription described above and using as an alternative prescription the pure MC values. The uncertainty on the trigger efficiency is negligible, due to the additional requirement on the single-muon transverse momentum which selects a p_T -region where the trigger efficiency is very high and its evaluation via data and MC is consistent. Finally, the procedure for the determination of the uncertainty related to the $\Upsilon(1S)$ kinematic distributions used in the MC is the same as for the J/ψ . The total systematic uncertainties for the $\Upsilon(1S)$ analysis are reported in Table 3, together with the results.

4 Results

The polarization parameters for J/ψ inclusive production in Pb–Pb collisions at $\sqrt{s_{NN}} = 5.02$ TeV in the helicity and Collins-Soper reference frames are shown in Fig. 3 and the corresponding numerical values are reported in Table 2. In Fig. 3, λ_θ , λ_ϕ and $\lambda_{\theta\phi}$ are also compared with the LHCb [24] and ALICE [23] measurements in pp collisions at $\sqrt{s} = 7$ and 8 TeV, respectively.

Table 2: J/ψ polarization parameters, measured for Pb–Pb collisions at $\sqrt{s_{NN}} = 5.02$ TeV, in the helicity and Collins-Soper reference frames in the rapidity interval $2.5 < y < 4$. The first uncertainty is statistical and the second systematic.

	p_T (GeV/c)	Helicity	Collins-Soper
λ_θ	$2 < p_T < 4$	$0.218 \pm 0.060 \pm 0.087$	$-0.157 \pm 0.049 \pm 0.058$
	$4 < p_T < 6$	$0.151 \pm 0.071 \pm 0.068$	$-0.057 \pm 0.059 \pm 0.055$
	$6 < p_T < 10$	$-0.070 \pm 0.068 \pm 0.047$	$-0.008 \pm 0.063 \pm 0.026$
λ_ϕ	$2 < p_T < 4$	$-0.029 \pm 0.017 \pm 0.031$	$0.061 \pm 0.015 \pm 0.033$
	$4 < p_T < 6$	$-0.013 \pm 0.019 \pm 0.036$	$0.047 \pm 0.024 \pm 0.023$
	$6 < p_T < 10$	$0.047 \pm 0.021 \pm 0.010$	$0.024 \pm 0.032 \pm 0.018$
$\lambda_{\theta\phi}$	$2 < p_T < 4$	$-0.124 \pm 0.028 \pm 0.043$	$-0.090 \pm 0.027 \pm 0.029$
	$4 < p_T < 6$	$-0.059 \pm 0.030 \pm 0.021$	$-0.040 \pm 0.034 \pm 0.046$
	$6 < p_T < 10$	$-0.025 \pm 0.031 \pm 0.030$	$0.018 \pm 0.035 \pm 0.044$

For all the p_T intervals and in both reference frames the values of the polarization parameters exhibit at most slight deviations from zero. In particular, $\lambda_\theta^{\text{HE}}$ indicates a slight transverse polarization at low p_T ($\sim 2.1\sigma$ effect, calculated using the Gaussian approximation), while $\lambda_\theta^{\text{CS}}$ shows a weak longitudinal polarization ($\sim 2.1\sigma$). When increasing p_T , the central values of λ_θ become close to zero. All values of λ_ϕ and $\lambda_{\theta\phi}$ are, in absolute value, smaller than 0.1, except for $\lambda_{\theta\phi}^{\text{HE}}$, which is -0.124 at low p_T and deviates from zero by $\sim 2.4\sigma$.

When comparing with the pp results, no significant difference is found with respect to ALICE results at $\sqrt{s} = 8$ TeV, which are compatible with zero. A significant difference is found with respect to the higher-precision LHCb results at $\sqrt{s} = 7$ TeV, reaching 3.3σ in the interval $2 < p_T < 4$ GeV/c in the helicity reference frame, where pp data [24] indicate a small but significant degree of longitudinal polarization, while the Pb–Pb results favor a slightly transverse polarization. In Pb–Pb collisions at LHC energies, a significant fraction of the detected J/ψ originates from the recombination of $c\bar{c}$ pairs in the QGP phase or when the system hadronizes. Moreover, the contribution from higher-mass charmonium states decaying

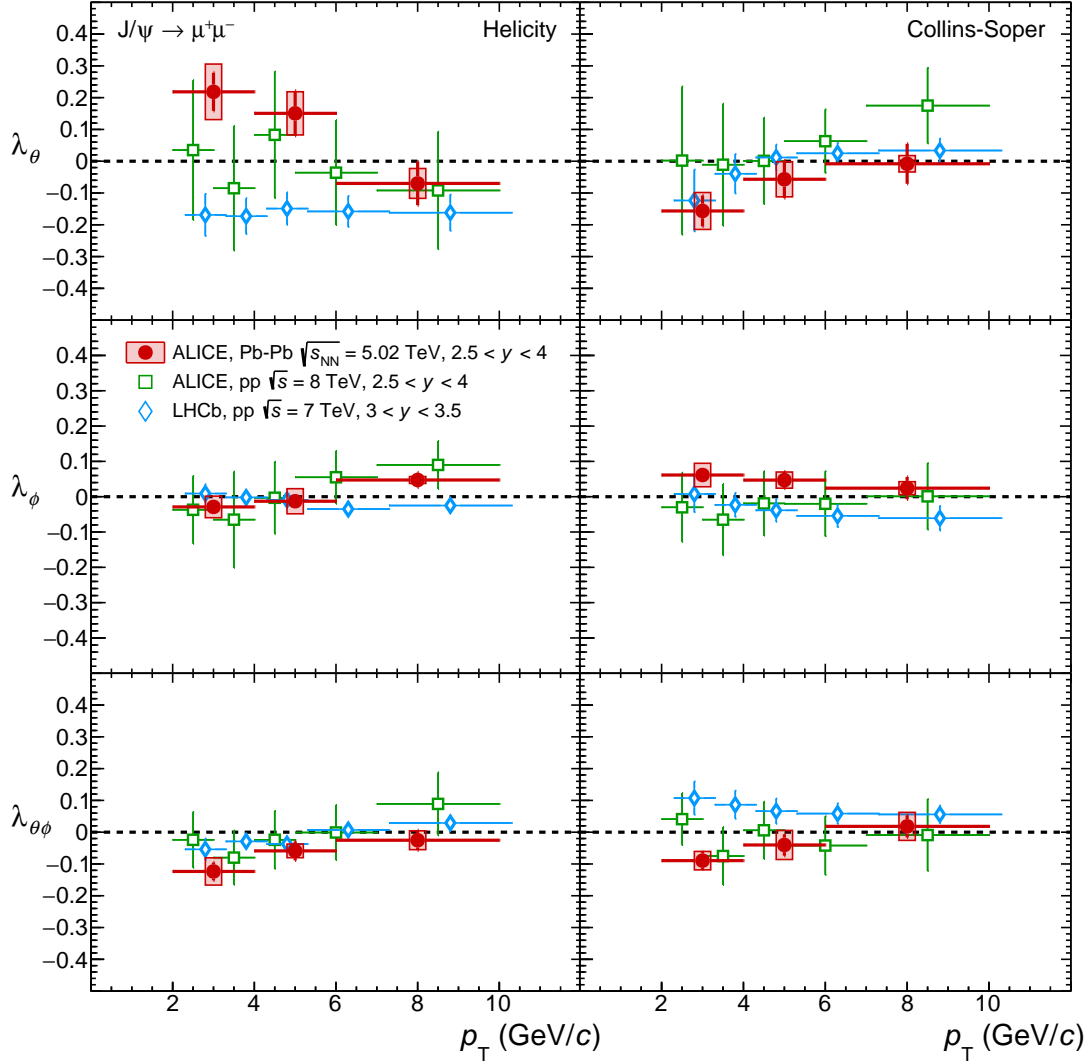


Figure 3: Inclusive J/ψ polarization parameters as a function of transverse momentum for Pb–Pb collisions at $\sqrt{s_{\text{NN}}} = 5.02$ TeV, compared with results obtained in pp collisions by ALICE at $\sqrt{s} = 8$ TeV [23] and by LHCb for prompt J/ψ at $\sqrt{s} = 7$ TeV [24] (the LHCb markers were shifted horizontally by +0.3 GeV/ c for better visibility) in the rapidity interval $3 < y < 3.5$. The error bars represent the total uncertainties for the pp results, while for Pb–Pb statistical and systematic uncertainties are plotted separately as a vertical bar and a shaded box, respectively. In the left part of the plot the polarization parameters in the helicity reference frame are reported, in the right those for the Collins-Soper frame.

to J/ψ could vary between pp and Pb–Pb due to different suppression effects for each state in nuclear collisions. Therefore, the observed hint for a different polarization in pp and Pb–Pb might be a reflection of the different production and suppression mechanisms in the two systems, but more precise data, along with quantitative theory estimates, are needed for a definite conclusion. It should also be noted that the ALICE results refer to inclusive production, while LHCb has measured prompt J/ψ . However, as discussed in Ref. [22], the size of the non-prompt component is small in the covered p_{T} region (of the order of 15% at high p_{T}) and its polarization was also measured to be small by CDF ($\lambda_{\theta}^{\text{HE}} \sim -0.1$ [21]), implying that the net effect of this source on inclusive J/ψ polarization should be negligible.

In Table 3 the values of the $\Upsilon(1S)$ polarization parameters are shown. The λ_θ values are consistent with zero, with large uncertainties that prevent a firm conclusion on the absence of polarization in nuclear collisions. The λ_ϕ and $\lambda_{\theta\phi}$ values are also consistent with zero. The relatively smaller uncertainties for these parameters are related to a more uniform acceptance distribution as a function of the azimuthal angular variable.

Table 3: $\Upsilon(1S)$ polarization parameters in the helicity and Collins-Soper reference frames measured in Pb–Pb collisions at $\sqrt{s_{NN}} = 5.02$ TeV in the rapidity interval $2.5 < y < 4$ and for transverse momentum $p_T < 15$ GeV/c. The first uncertainty is statistical and the second systematic.

	Helicity	Collins-Soper
λ_θ	$-0.090 \pm 0.395 \pm 0.101$	$0.418 \pm 0.526 \pm 0.178$
λ_ϕ	$-0.094 \pm 0.072 \pm 0.020$	$-0.141 \pm 0.087 \pm 0.033$
$\lambda_{\theta\phi}$	$-0.074 \pm 0.099 \pm 0.020$	$0.017 \pm 0.113 \pm 0.024$

5 Conclusions

The first measurement of the polarization parameters for J/ψ production in nuclear collisions at LHC energies was carried out by the ALICE Collaboration in Pb–Pb interactions at $\sqrt{s_{NN}} = 5.02$ TeV. The λ_θ , λ_ϕ and $\lambda_{\theta\phi}$ parameters were evaluated in the helicity and Collins-Soper reference frames in the rapidity interval $2.5 < y < 4$ and in the transverse momentum interval $2 < p_T < 10$ GeV/c. All the parameter values are close to zero, with a $\sim 2.1\sigma$ indication for a small transverse polarization in the helicity frame at low p_T , and a corresponding indication for a small longitudinal polarization in the Collins-Soper frame ($\sim 2.1\sigma$ effect). When comparing these results with pp data taken at higher energy at the LHC, an interesting feature is a significant difference in $\lambda_\theta^{\text{HE}}$ with respect to the LHCb results which showed instead a small longitudinal polarization in a similar kinematic domain. This first result obtained for J/ψ in nuclear collisions and described in this Letter represents therefore a starting point for future studies connecting such features with the known differences in the production mechanisms between pp and nucleus–nucleus collisions. Results were also obtained for the first time for the $\Upsilon(1S)$ polarization, integrated over p_T and y , showing, within the large uncertainties of the measurement, values compatible with the absence of polarization.

Acknowledgements

The ALICE Collaboration would like to thank all its engineers and technicians for their invaluable contributions to the construction of the experiment and the CERN accelerator teams for the outstanding performance of the LHC complex. The ALICE Collaboration gratefully acknowledges the resources and support provided by all Grid centres and the Worldwide LHC Computing Grid (WLCG) collaboration. The ALICE Collaboration acknowledges the following funding agencies for their support in building and running the ALICE detector: A. I. Alikhanyan National Science Laboratory (Yerevan Physics Institute) Foundation (ANSL), State Committee of Science and World Federation of Scientists (WFS), Armenia; Austrian Academy of Sciences, Austrian Science Fund (FWF): [M 2467-N36] and Nationalstiftung für Forschung, Technologie und Entwicklung, Austria; Ministry of Communications and High Technologies, National Nuclear Research Center, Azerbaijan; Conselho Nacional de Desenvolvimento Científico e Tecnológico (CNPq), Financiadora de Estudos e Projetos (Finep), Fundação de Amparo à Pesquisa do Estado de São Paulo (FAPESP) and Universidade Federal do Rio Grande do Sul (UFRGS), Brazil; Ministry of Education of China (MOEC), Ministry of Science & Technology of China (MSTC) and National Natural Science Foundation of China (NSFC), China; Ministry of Science and Education and Croatian Science Foundation, Croatia; Centro de Aplicaciones Tecnológicas y Desarrollo Nuclear

(CEADEN), Cubaenergía, Cuba; Ministry of Education, Youth and Sports of the Czech Republic, Czech Republic; The Danish Council for Independent Research | Natural Sciences, the VILLUM FONDEN and Danish National Research Foundation (DNRF), Denmark; Helsinki Institute of Physics (HIP), Finland; Commissariat à l’Energie Atomique (CEA) and Institut National de Physique Nucléaire et de Physique des Particules (IN2P3) and Centre National de la Recherche Scientifique (CNRS), France; Bundesministerium für Bildung und Forschung (BMBF) and GSI Helmholtzzentrum für Schwerionenforschung GmbH, Germany; General Secretariat for Research and Technology, Ministry of Education, Research and Religions, Greece; National Research, Development and Innovation Office, Hungary; Department of Atomic Energy Government of India (DAE), Department of Science and Technology, Government of India (DST), University Grants Commission, Government of India (UGC) and Council of Scientific and Industrial Research (CSIR), India; Indonesian Institute of Science, Indonesia; Centro Fermi - Museo Storico della Fisica e Centro Studi e Ricerche Enrico Fermi and Istituto Nazionale di Fisica Nucleare (INFN), Italy; Institute for Innovative Science and Technology, Nagasaki Institute of Applied Science (IIST), Japanese Ministry of Education, Culture, Sports, Science and Technology (MEXT) and Japan Society for the Promotion of Science (JSPS) KAKENHI, Japan; Consejo Nacional de Ciencia (CONACYT) y Tecnología, through Fondo de Cooperación Internacional en Ciencia y Tecnología (FONCICYT) and Dirección General de Asuntos del Personal Académico (DGAPA), Mexico; Nederlandse Organisatie voor Wetenschappelijk Onderzoek (NWO), Netherlands; The Research Council of Norway, Norway; Commission on Science and Technology for Sustainable Development in the South (COMSATS), Pakistan; Pontificia Universidad Católica del Perú, Peru; Ministry of Science and Higher Education, National Science Centre and WUT ID-UB, Poland; Korea Institute of Science and Technology Information and National Research Foundation of Korea (NRF), Republic of Korea; Ministry of Education and Scientific Research, Institute of Atomic Physics and Ministry of Research and Innovation and Institute of Atomic Physics, Romania; Joint Institute for Nuclear Research (JINR), Ministry of Education and Science of the Russian Federation, National Research Centre Kurchatov Institute, Russian Science Foundation and Russian Foundation for Basic Research, Russia; Ministry of Education, Science, Research and Sport of the Slovak Republic, Slovakia; National Research Foundation of South Africa, South Africa; Swedish Research Council (VR) and Knut & Alice Wallenberg Foundation (KAW), Sweden; European Organization for Nuclear Research, Switzerland; Suranaree University of Technology (SUT), National Science and Technology Development Agency (NSDTA) and Office of the Higher Education Commission under NRU project of Thailand, Thailand; Turkish Atomic Energy Agency (TAEK), Turkey; National Academy of Sciences of Ukraine, Ukraine; Science and Technology Facilities Council (STFC), United Kingdom; National Science Foundation of the United States of America (NSF) and United States Department of Energy, Office of Nuclear Physics (DOE NP), United States of America.

References

- [1] **Particle Data Group** Collaboration, M. Tanabashi *et al.*, “Review of Particle Physics,” *Phys. Rev.* **D98** no. 3, (2018) 030001.
- [2] G. T. Bodwin, E. Braaten, and G. P. Lepage, “Rigorous QCD analysis of inclusive annihilation and production of heavy quarkonium,” *Phys. Rev.* **D51** (1995) 1125–1171, arXiv:hep-ph/9407339 [hep-ph]. [Erratum: *Phys. Rev.*D55,5853(1997)].
- [3] **ALICE** Collaboration, S. Acharya *et al.*, “Energy dependence of forward-rapidity J/ψ and $\psi(2S)$ production in pp collisions at the LHC,” *Eur. Phys. J.* **C77** no. 6, (2017) 392, arXiv:1702.00557 [hep-ex].
- [4] **ALICE** Collaboration, S. Acharya *et al.*, “Inclusive J/ψ production at mid-rapidity in pp collisions at $\sqrt{s} = 5.02$ TeV,” *JHEP* **10** (2019) 084, arXiv:1905.07211 [nucl-ex].

- [5] **LHCb** Collaboration, R. Aaij *et al.*, “Measurement of forward J/ψ production cross-sections in pp collisions at $\sqrt{s} = 13$ TeV,” *JHEP* **10** (2015) 172, arXiv:1509.00771 [hep-ex]. [Erratum: JHEP05,063(2017)].
- [6] **CMS** Collaboration, A. M. Sirunyan *et al.*, “Measurement of quarkonium production cross sections in pp collisions at $\sqrt{s} = 13$ TeV,” *Phys. Lett.* **B780** (2018) 251–272, arXiv:1710.11002 [hep-ex].
- [7] **ATLAS** Collaboration, G. Aad *et al.*, “Measurement of the differential cross-sections of prompt and non-prompt production of J/ψ and $\psi(2S)$ in pp collisions at $\sqrt{s} = 7$ and 8 TeV with the ATLAS detector,” *Eur. Phys. J.* **C76** no. 5, (2016) 283, arXiv:1512.03657 [hep-ex].
- [8] **PHENIX** Collaboration, U. Acharya *et al.*, “ J/ψ and $\psi(2S)$ production at forward rapidity in $p+p$ collisions at $\sqrt{s} = 510$ GeV,” *Phys. Rev. D* **101** no. 5, (2020) 052006, arXiv:1912.13424 [hep-ex].
- [9] **STAR** Collaboration, J. Adam *et al.*, “Measurements of the transverse-momentum-dependent cross sections of J/ψ production at mid-rapidity in proton+proton collisions at $\sqrt{s} = 510$ and 500 GeV with the STAR detector,” *Phys. Rev.* **D100** no. 5, (2019) 052009, arXiv:1905.06075 [hep-ex].
- [10] **CDF** Collaboration, F. Abe *et al.*, “ J/ψ and $\psi(2S)$ production in $p\bar{p}$ collisions at $\sqrt{s} = 1.8$ TeV,” *Phys. Rev. Lett.* **79** (1997) 572–577.
- [11] **D0** Collaboration, S. Abachi *et al.*, “ J/ψ production in $p\bar{p}$ collisions at $\sqrt{s} = 1.8$ -TeV,” *Phys. Lett.* **B370** (1996) 239–248.
- [12] **LHCb** Collaboration, R. Aaij *et al.*, “Measurement of Υ production in pp collisions at $\sqrt{s} = 13$ TeV,” *JHEP* **07** (2018) 134, arXiv:1804.09214 [hep-ex]. [Erratum: JHEP05,076(2019)].
- [13] **ALICE** Collaboration, J. Adam *et al.*, “Inclusive quarkonium production at forward rapidity in pp collisions at $\sqrt{s} = 8$ TeV,” *Eur. Phys. J.* **C76** no. 4, (2016) 184, arXiv:1509.08258 [hep-ex].
- [14] **ATLAS** Collaboration, G. Aad *et al.*, “Measurement of Upsilon production in 7 TeV pp collisions at ATLAS,” *Phys. Rev.* **D87** no. 5, (2013) 052004, arXiv:1211.7255 [hep-ex].
- [15] M. Einhorn and S. Ellis, “Hadronic Production of the New Resonances: Probing Gluon Distributions,” *Phys. Rev. D* **12** (1975) 2007.
- [16] M. Gluck, J. F. Owens, and E. Reya, “Gluon Contribution to Hadronic J/ψ Production,” *Phys. Rev.* **D17** (1978) 2324.
- [17] S. Baranov and A. Lipatov, “Prompt charmonia production and polarization at LHC in the NRQCD with k_T -factorization. Part III: J/ψ meson,” *Phys. Rev. D* **96** no. 3, (2017) 034019, arXiv:1611.10141 [hep-ph].
- [18] E. Braaten, B. A. Kniehl, and J. Lee, “Polarization of prompt J/ψ at the Tevatron,” *Phys. Rev.* **D62** (2000) 094005, arXiv:hep-ph/9911436 [hep-ph].
- [19] P. Faccioli, C. Lourenco, J. Seixas, and H. K. Wohri, “Towards the experimental clarification of quarkonium polarization,” *Eur. Phys. J.* **C69** (2010) 657–673, arXiv:1006.2738 [hep-ph].
- [20] **CDF** Collaboration, T. Affolder *et al.*, “Measurement of J/ψ and $\psi(2S)$ polarization in $p\bar{p}$ collisions at $\sqrt{s} = 1.8$ TeV,” *Phys. Rev. Lett.* **85** (2000) 2886–2891, arXiv:hep-ex/0004027 [hep-ex].

- [21] **CDF** Collaboration, A. Abulencia *et al.*, “Polarization of J/ψ and $\psi(2S)$ Mesons Produced in $p\bar{p}$ Collisions at $\sqrt{s} = 1.96$ -TeV,” *Phys. Rev. Lett.* **99** (2007) 132001, arXiv:0704.0638 [hep-ex].
- [22] **ALICE** Collaboration, B. Abelev *et al.*, “ J/ψ polarization in pp collisions at $\sqrt{s} = 7$ TeV,” *Phys. Rev. Lett.* **108** (2012) 082001, arXiv:1111.1630 [hep-ex].
- [23] **ALICE** Collaboration, S. Acharya *et al.*, “Measurement of the inclusive J/ψ polarization at forward rapidity in pp collisions at $\sqrt{s} = 8$ TeV,” *Eur. Phys. J.* **C78** no. 7, (2018) 562, arXiv:1805.04374 [hep-ex].
- [24] **LHCb** Collaboration, R. Aaij *et al.*, “Measurement of J/ψ polarization in pp collisions at $\sqrt{s} = 7$ TeV,” *Eur. Phys. J.* **C73** no. 11, (2013) 2631, arXiv:1307.6379 [hep-ex].
- [25] **CMS** Collaboration, S. Chatrchyan *et al.*, “Measurement of the Prompt J/ψ and $\psi(2S)$ Polarizations in pp Collisions at $\sqrt{s} = 7$ TeV,” *Phys. Lett.* **B727** (2013) 381–402, arXiv:1307.6070 [hep-ex].
- [26] M. Butenschoen and B. A. Kniehl, “Reconciling J/ψ production at HERA, RHIC, Tevatron, and LHC with NRQCD factorization at next-to-leading order,” *Phys. Rev. Lett.* **106** (2011) 022003, arXiv:1009.5662 [hep-ph].
- [27] Y.-Q. Ma, K. Wang, and K.-T. Chao, “A complete NLO calculation of the J/ψ and ψ' production at hadron colliders,” *Phys. Rev.* **D84** (2011) 114001, arXiv:1012.1030 [hep-ph].
- [28] M. Butenschoen and B. A. Kniehl, “ J/ψ polarization at Tevatron and LHC: Nonrelativistic-QCD factorization at the crossroads,” *Phys. Rev. Lett.* **108** (2012) 172002, arXiv:1201.1872 [hep-ph].
- [29] K.-T. Chao, Y.-Q. Ma, H.-S. Shao, K. Wang, and Y.-J. Zhang, “ J/ψ Polarization at Hadron Colliders in Nonrelativistic QCD,” *Phys. Rev. Lett.* **108** (2012) 242004, arXiv:1201.2675 [hep-ph].
- [30] B. Gong, L.-P. Wan, J.-X. Wang, and H.-F. Zhang, “Polarization for Prompt J/ψ and $\psi(2s)$ Production at the Tevatron and LHC,” *Phys. Rev. Lett.* **110** no. 4, (2013) 042002, arXiv:1205.6682 [hep-ph].
- [31] Y. Feng, B. Gong, C.-H. Chang, and J.-X. Wang, “Remaining parts of the long-standing J/ψ polarization puzzle,” *Phys. Rev.* **D99** no. 1, (2019) 014044, arXiv:1810.08989 [hep-ph].
- [32] Y.-Q. Ma, T. Stebel, and R. Venugopalan, “ J/ψ polarization in the CGC+NRQCD approach,” *JHEP* **12** (2018) 057, arXiv:1809.03573 [hep-ph].
- [33] **CMS** Collaboration, S. Chatrchyan *et al.*, “Measurement of the $\Upsilon(1S)$, $\Upsilon(2S)$ and $\Upsilon(3S)$ polarizations in pp collisions at $\sqrt{s} = 7$ TeV,” *Phys. Rev. Lett.* **110** no. 8, (2013) 081802, arXiv:1209.2922 [hep-ex].
- [34] **CMS** Collaboration, V. Khachatryan *et al.*, “ $\Upsilon(nS)$ polarizations versus particle multiplicity in pp collisions at $\sqrt{s} = 7$ TeV,” *Phys. Lett. B* **761** (2016) 31–52, arXiv:1603.02913 [hep-ex].
- [35] **LHCb** Collaboration, R. Aaij *et al.*, “Measurement of the Υ polarizations in pp collisions at $\sqrt{s} = 7$ and 8 TeV,” *JHEP* **12** (2017) 110, arXiv:1709.01301 [hep-ex].
- [36] H. Han, Y.-Q. Ma, C. Meng, H.-S. Shao, Y.-J. Zhang, and K.-T. Chao, “ $\Upsilon(nS)$ and $\chi_b(nP)$ production at hadron colliders in nonrelativistic QCD,” *Phys. Rev.* **D94** no. 1, (2016) 014028, arXiv:1410.8537 [hep-ph].

- [37] P. Braun-Munzinger and J. Wambach, “The Phase Diagram of Strongly-Interacting Matter,” *Rev. Mod. Phys.* **81** (2009) 1031–1050, arXiv:0801.4256 [hep-ph].
- [38] P. Braun-Munzinger, V. Koch, T. Schäfer, and J. Stachel, “Properties of hot and dense matter from relativistic heavy ion collisions,” *Phys. Rept.* **621** (2016) 76–126, arXiv:1510.00442 [nucl-th].
- [39] T. Matsui and H. Satz, “ J/ψ Suppression by Quark-Gluon Plasma Formation,” *Phys. Lett.* **B178** (1986) 416–422.
- [40] M. Laine, “A Resummed perturbative estimate for the quarkonium spectral function in hot QCD,” *JHEP* **05** (2007) 028, arXiv:0704.1720 [hep-ph].
- [41] P. Braun-Munzinger and J. Stachel, “(Non)thermal aspects of charmonium production and a new look at J/ψ suppression,” *Phys. Lett.* **B490** (2000) 196–202, arXiv:nucl-th/0007059 [nucl-th].
- [42] R. L. Thews, M. Schroedter, and J. Rafelski, “Enhanced J/ψ production in deconfined quark matter,” *Phys. Rev.* **C63** (2001) 054905, arXiv:hep-ph/0007323 [hep-ph].
- [43] B. L. Ioffe and D. E. Kharzeev, “Quarkonium polarization in heavy ion collisions as a possible signature of the quark gluon plasma,” *Phys. Rev.* **C68** (2003) 061902, arXiv:hep-ph/0306176 [hep-ph].
- [44] H.-S. Shao, Y.-Q. Ma, K. Wang, and K.-T. Chao, “Polarizations of χ_{c1} and χ_{c2} in prompt production at the LHC,” *Phys. Rev. Lett.* **112** no. 18, (2014) 182003, arXiv:1402.2913 [hep-ph].
- [45] CMS Collaboration, A. M. Sirunyan *et al.*, “Measurement of the χ_{c1} and χ_{c2} polarizations in proton-proton collisions at $\sqrt{s} = 8$ TeV,” arXiv:1912.07706 [hep-ex].
- [46] ALICE Collaboration, K. Aamodt *et al.*, “The ALICE experiment at the CERN LHC,” *JINST* **3** (2008) S08002.
- [47] ALICE Collaboration, B. Abelev *et al.*, “Performance of the ALICE Experiment at the CERN LHC,” *Int. J. Mod. Phys.* **A29** (2014) 1430044, arXiv:1402.4476 [nucl-ex].
- [48] ALICE Collaboration, K. Aamodt *et al.*, “Rapidity and transverse momentum dependence of inclusive J/ψ production in pp collisions at $\sqrt{s} = 7$ TeV,” *Phys. Lett.* **B704** (2011) 442, arXiv:1105.0380 [hep-ex].
- [49] ALICE Collaboration, E. Abbas *et al.*, “Performance of the ALICE VZERO system,” *JINST* **8** (2013) P10016, arXiv:1306.3130 [nucl-ex].
- [50] ALICE Collaboration, K. Aamodt *et al.*, “Alignment of the ALICE Inner Tracking System with cosmic-ray tracks,” *JINST* **5** (2010) P03003, arXiv:1001.0502 [physics.ins-det].
- [51] ALICE Collaboration, B. Abelev *et al.*, “Measurement of the Cross Section for Electromagnetic Dissociation with Neutron Emission in Pb-Pb Collisions at $\sqrt{s_{NN}} = 2.76$ TeV,” *Phys. Rev. Lett.* **109** (2012) 252302, arXiv:1203.2436 [nucl-ex].
- [52] ALICE Collaboration, F. Bossu, M. Gagliardi, and M. Marchisone, “Performance of the RPC-based ALICE muon trigger system at the LHC,” *JINST* **7** (2012) T12002, arXiv:1211.1948 [physics.ins-det]. [PoSRPC2012,059(2012)].

- [53] **ALICE** Collaboration, B. Abelev *et al.*, “Centrality determination of Pb-Pb collisions at $\sqrt{s_{\text{NN}}} = 2.76$ TeV with ALICE,” *Phys. Rev.* **C88** no. 4, (2013) 044909, arXiv:1301.4361 [nucl-ex].
- [54] **ALICE** Collaboration, “Centrality determination in heavy ion collisions,” ALICE-PUBLIC-2018-011. <http://cds.cern.ch/record/2636623>.
- [55] **ALICE** Collaboration, “Quarkonium signal extraction in ALICE,” ALICE-PUBLIC-2015-006. <https://cds.cern.ch/record/2060096>.
- [56] **ALICE** Collaboration, S. Acharya *et al.*, “Studies of J/ψ production at forward rapidity in Pb-Pb collisions at $\sqrt{s_{\text{NN}}} = 5.02$ TeV,” *JHEP* **02** (2020) 041, arXiv:1909.03158 [nucl-ex].
- [57] **ALICE** Collaboration, S. Acharya *et al.*, “Inclusive J/ψ production at forward and backward rapidity in p-Pb collisions at $\sqrt{s_{\text{NN}}} = 8.16$ TeV,” *JHEP* **07** (2018) 160, arXiv:1805.04381 [nucl-ex].
- [58] R. Brun, F. Bruyant, F. Carminati, S. Giani, M. Maire, A. McPherson, G. Patrick, and L. Urban, *GEANT: Detector Description and Simulation Tool; Oct 1994*. CERN Program Library. CERN, Geneva, 1993. <http://cds.cern.ch/record/1082634>. Long Writeup W5013.
- [59] **ALICE** Collaboration, B. Abelev *et al.*, “Measurement of quarkonium production at forward rapidity in pp collisions at $\sqrt{s} = 7$ TeV,” *Eur. Phys. J.* **C74** no. 8, (2014) 2974, arXiv:1403.3648 [nucl-ex].
- [60] **ALICE** Collaboration, S. Acharya *et al.*, “ Υ suppression at forward rapidity in Pb-Pb collisions at $\sqrt{s_{\text{NN}}} = 5.02$ TeV,” *Phys. Lett.* **B790** (2019) 89–101, arXiv:1805.04387 [nucl-ex].

A The ALICE Collaboration

S. Acharya¹⁴¹, D. Adamová⁹⁵, A. Adler⁷⁴, J. Adolfsson⁸¹, M.M. Aggarwal¹⁰⁰, G. Aglieri Rinella³⁴, M. Agnello³⁰, N. Agrawal^{10,54}, Z. Ahmed¹⁴¹, S. Ahmad¹⁶, S.U. Ahn⁷⁶, Z. Akbar⁵¹, A. Akindinov⁹², M. Al-Turany¹⁰⁷, S.N. Alam^{40,141}, D.S.D. Albuquerque¹²², D. Aleksandrov⁸⁸, B. Alessandro⁵⁹, H.M. Alfanda⁶, R. Alfaro Molina⁷¹, B. Ali¹⁶, Y. Ali¹⁴, A. Alici^{10,26,54}, N. Alizadehvandchali¹²⁵, A. Alkin^{2,34}, J. Alme²¹, T. Alt⁶⁸, L. Altenkamper²¹, I. Altsybeev¹¹³, M.N. Anaam⁶, C. Andrei⁴⁸, D. Andreou³⁴, A. Andronic¹⁴⁴, M. Angeletti³⁴, V. Anguelov¹⁰⁴, C. Anson¹⁵, T. Antičić¹⁰⁸, F. Antinori⁵⁷, P. Antonioli⁵⁴, N. Apadula⁸⁰, L. Aphecetche¹¹⁵, H. Appelshäuser⁶⁸, S. Arcelli²⁶, R. Arnaldi⁵⁹, M. Arratia⁸⁰, I.C. Arsene²⁰, M. Arslanovic¹⁰⁴, A. Augustinus³⁴, R. Averbeck¹⁰⁷, S. Aziz⁷⁸, M.D. Azmi¹⁶, A. Badalá⁵⁶, Y.W. Baek⁴¹, S. Bagnasco⁵⁹, X. Bai¹⁰⁷, R. Bailhache⁶⁸, R. Bala¹⁰¹, A. Balbino³⁰, A. Baldisseri¹³⁷, M. Ball⁴³, S. Balouza¹⁰⁵, D. Banerjee³, R. Barbera²⁷, L. Barioglio²⁵, G.G. Barnaföldi¹⁴⁵, L.S. Barnby⁹⁴, V. Barret¹³⁴, P. Bartalini⁶, C. Bartels¹²⁷, K. Barth³⁴, E. Bartsch⁶⁸, F. Baruffaldi²⁸, N. Bastid¹³⁴, S. Basu¹⁴³, G. Batigne¹¹⁵, B. Batyunya⁷⁵, D. Bauri⁴⁹, J.L. Bazo Alba¹¹², I.G. Bearden⁸⁹, C. Beattie¹⁴⁶, C. Bedda⁶³, N.K. Behera⁶¹, I. Belikov¹³⁶, A.D.C. Bell Hechavarria¹⁴⁴, F. Bellini³⁴, R. Bellwied¹²⁵, V. Belyaev⁹³, G. Bencedi¹⁴⁵, S. Beole²⁵, A. Bercuci⁴⁸, Y. Berdnikov⁹⁸, D. Berenyi¹⁴⁵, R.A. Bertens¹³⁰, D. Berzano⁵⁹, M.G. Besoiu⁶⁷, L. Betev³⁴, A. Bhasin¹⁰¹, I.R. Bhat¹⁰¹, M.A. Bhat³, H. Bhatt⁴⁹, B. Bhattacharjee⁴², A. Bianchi²⁵, L. Bianchi²⁵, N. Bianchi⁵², J. Bielčik³⁷, J. Bielčiková⁹⁵, A. Bilandzic¹⁰⁵, G. Biro¹⁴⁵, R. Biswas³, S. Biswas³, J.T. Blair¹¹⁹, D. Blau⁸⁸, C. Blume⁶⁸, G. Boca¹³⁹, F. Bock⁹⁶, A. Bogdanov⁹³, S. Boi²³, J. Bok⁶¹, L. Boldizsár¹⁴⁵, A. Bolozdynya⁹³, M. Bombara³⁸, G. Bonomi¹⁴⁰, H. Borel¹³⁷, A. Borissov⁹³, H. Bossi¹⁴⁶, E. Botta²⁵, L. Bratrud⁶⁸, P. Braun-Munzinger¹⁰⁷, M. Bregant¹²¹, M. Broz³⁷, E. Bruna⁵⁹, G.E. Bruno^{33,106}, M.D. Buckland¹²⁷, D. Budnikov¹⁰⁹, H. Buesching⁶⁸, S. Bufalino³⁰, O. Bugnon¹¹⁵, P. Buhler¹¹⁴, P. Buncic³⁴, Z. Buthelezi^{72,131}, J.B. Butt¹⁴, S.A. Bysiak¹¹⁸, D. Caffarri⁹⁰, M. Cai⁶, A. Caliva¹⁰⁷, E. Calvo Villar¹¹², J.M.M. Camacho¹²⁰, R.S. Camacho⁴⁵, P. Camerini²⁴, F.D.M. Canedo¹²¹, A.A. Capon¹¹⁴, F. Carnesecchi²⁶, R. Caron¹³⁷, J. Castillo Castellanos¹³⁷, A.J. Castro¹³⁰, E.A.R. Casula⁵⁵, F. Catalano³⁰, C. Ceballos Sanchez⁷⁵, P. Chakraborty⁴⁹, S. Chandra¹⁴¹, W. Chang⁶, S. Chapeland³⁴, M. Chartier¹²⁷, S. Chattopadhyay¹⁴¹, S. Chattopadhyay¹¹⁰, A. Chauvin²³, C. Cheshkov¹³⁵, B. Cheynis¹³⁵, V. Chibante Barroso³⁴, D.D. Chinellato¹²², S. Cho⁶¹, P. Chochula³⁴, T. Chowdhury¹³⁴, P. Christakoglou⁹⁰, C.H. Christensen⁸⁹, P. Christiansen⁸¹, T. Chujo¹³³, C. Cicalo⁵⁵, L. Cifarelli^{10,26}, L.D. Cilladi²⁵, F. Cindolo⁵⁴, M.R. Ciupek¹⁰⁷, G. Clai^{54,ii}, J. Cleymans¹²⁴, F. Colamaria⁵³, D. Colella⁵³, A. Collu⁸⁰, M. Colocci²⁶, M. Concas^{59,iii}, G. Conesa Balbastre⁷⁹, Z. Conesa del Valle⁷⁸, G. Contin^{24,60}, J.G. Contreras³⁷, T.M. Cormier⁹⁶, Y. Corrales Morales²⁵, P. Cortese³¹, M.R. Cosentino¹²³, F. Costa³⁴, S. Costanza¹³⁹, P. Crochet¹³⁴, E. Cuautle⁶⁹, P. Cui⁶, L. Cunqueiro⁹⁶, D. Dabrowski¹⁴², T. Dahms¹⁰⁵, A. Dainese⁵⁷, F.P.A. Damas^{115,137}, M.C. Danisch¹⁰⁴, A. Danu⁶⁷, D. Das¹¹⁰, I. Das¹¹⁰, P. Das⁸⁶, P. Das³, S. Das³, A. Dash⁸⁶, S. Dash⁴⁹, S. De⁸⁶, A. De Caro²⁹, G. de Cataldo⁵³, J. de Cuveland³⁹, A. De Falco²³, D. De Gruttola¹⁰, N. De Marco⁵⁹, S. De Pasquale²⁹, S. Deb⁵⁰, H.F. Degenhardt¹²¹, K.R. Deja¹⁴², A. Deloff⁸⁵, S. Delsanto^{25,131}, W. Deng⁶, P. Dhankher⁴⁹, D. Di Bari³³, A. Di Mauro³⁴, R.A. Diaz⁸, T. Dietel¹²⁴, P. Dillenseger⁶⁸, Y. Ding⁶, R. Divia³⁴, D.U. Dixit¹⁹, Ø. Djuvsland²¹, U. Dmitrieva⁶², A. Dobrin⁶⁷, B. Dönigus⁶⁸, O. Dordic²⁰, A.K. Dubey¹⁴¹, A. Dubla^{90,107}, S. Dudi¹⁰⁰, M. Dukhishyam⁸⁶, P. Dupieux¹³⁴, R.J. Ehlers⁹⁶, V.N. Eikeland²¹, D. Elia⁵³, B. Erazmus¹¹⁵, F. Erhardt⁹⁹, A. Erokhin¹¹³, M.R. Ersdal²¹, B. Espagnon⁷⁸, G. Eulisse³⁴, D. Evans¹¹¹, S. Evdokimov⁹¹, L. Fabbietti¹⁰⁵, M. Faggin²⁸, J. Faivre⁷⁹, F. Fan⁶, A. Fantoni⁵², M. Fasel⁹⁶, P. Fedichio³⁰, A. Feliciello⁵⁹, G. Feofilov¹¹³, A. Fernández Téllez⁴⁵, A. Ferrero¹³⁷, A. Ferretti²⁵, A. Festanti³⁴, V.J.G. Feuillard¹⁰⁴, J. Figiel¹¹⁸, S. Filchagin¹⁰⁹, D. Finogeev⁶², F.M. Fionda²¹, G. Fiorenza⁵³, F. Flor¹²⁵, A.N. Flores¹¹⁹, S. Foertsch⁷², P. Foka¹⁰⁷, S. Fokin⁸⁸, E. Fragiaco⁶⁰, U. Frankenfeld¹⁰⁷, U. Fuchs³⁴, C. Furget⁷⁹, A. Furs⁶², M. Fusco Girard²⁹, J.J. Gaardhøje⁸⁹, M. Gagliardi²⁵, A.M. Gago¹¹², A. Gal¹³⁶, C.D. Galvan¹²⁰, P. Ganotti⁸⁴, C. Garabatos¹⁰⁷, J.R.A. Garcia⁴⁵, E. Garcia-Solis¹¹, K. Garg¹¹⁵, C. Gargiulo³⁴, A. Garibli⁸⁷, K. Garner¹⁴⁴, P. Gasik^{105,107}, E.F. Gauger¹¹⁹, M.B. Gay Ducati⁷⁰, M. Germain¹¹⁵, J. Ghosh¹¹⁰, P. Ghosh¹⁴¹, S.K. Ghosh³, M. Giacalone²⁶, P. Gianotti⁵², P. Giubellino^{59,107}, P. Giubileo²⁸, A.M.C. Glaenzer¹³⁷, P. Glässel¹⁰⁴, A. Gomez Ramirez⁷⁴, V. Gonzalez^{107,143}, L.H. González-Trueba⁷¹, S. Gorbunov³⁹, L. Görlich¹¹⁸, A. Goswami⁴⁹, S. Gotovac³⁵, V. Grabski⁷¹, L.K. Graczykowski¹⁴², K.L. Graham¹¹¹, L. Greiner⁸⁰, A. Grelli⁶³, C. Grigoras³⁴, V. Grigoriev⁹³, A. Grigoryan¹, S. Grigoryan⁷⁵, O.S. Groettvik²¹, F. Grosa^{30,59}, J.F. Grosse-Oetringhaus³⁴, R. Grosso¹⁰⁷, R. Guernane⁷⁹, M. Guittiere¹¹⁵, K. Gulbrandsen⁸⁹, T. Gunji¹³², A. Gupta¹⁰¹, R. Gupta¹⁰¹, I.B. Guzman⁴⁵, R. Haake¹⁴⁶, M.K. Habib¹⁰⁷, C. Hadjidakis⁷⁸, H. Hamagaki⁸², G. Hamar¹⁴⁵, M. Hamid⁶, R. Hannigan¹¹⁹, M.R. Haque^{63,86}, A. Harlanderova¹⁰⁷, J.W. Harris¹⁴⁶, A. Harton¹¹, J.A. Hasenbichler³⁴, H. Hassan⁹⁶, Q.U. Hassan¹⁴, D. Hatzifotiadou^{10,54}, P. Hauer⁴³, L.B. Havener¹⁴⁶, S. Hayashi¹³², S.T. Heckel¹⁰⁵, E. Hellbär⁶⁸, H. Helstrup³⁶, A. Herghelegiu⁴⁸, T. Herman³⁷, E.G. Hernandez⁴⁵, G. Herrera Corral⁹, F. Herrmann¹⁴⁴, K.F. Hetland³⁶, H. Hillemanns³⁴, C. Hills¹²⁷, B. Hippolyte¹³⁶, B. Hohlweger¹⁰⁵,

J. Honermann¹⁴⁴, D. Horak³⁷, A. Hornung⁶⁸, S. Hornung¹⁰⁷, R. Hosokawa^{15,133}, P. Hristov³⁴, C. Huang⁷⁸, C. Hughes¹³⁰, P. Huhn⁶⁸, T.J. Humanic⁹⁷, H. Hushnud¹¹⁰, L.A. Husova¹⁴⁴, N. Hussain⁴², S.A. Hussain¹⁴, D. Hutter³⁹, J.P. Iddon^{34,127}, R. Ilkaev¹⁰⁹, H. Ilyas¹⁴, M. Inaba¹³³, G.M. Innocenti³⁴, M. Ippolitov⁸⁸, A. Isakov⁹⁵, M.S. Islam¹¹⁰, M. Ivanov¹⁰⁷, V. Ivanov⁹⁸, V. Izucheev⁹¹, B. Jacak⁸⁰, N. Jacazio^{34,54}, P.M. Jacobs⁸⁰, S. Jadlovská¹¹⁷, J. Jadlovsky¹¹⁷, S. Jaelani⁶³, C. Jahnke¹²¹, M.J. Jakubowska¹⁴², M.A. Janik¹⁴², T. Janson⁷⁴, M. Jercic⁹⁹, O. Jevons¹¹¹, M. Jin¹²⁵, F. Jonas^{96,144}, P.G. Jones¹¹¹, J. Jung⁶⁸, M. Jung⁶⁸, A. Jusko¹¹¹, P. Kalinak⁶⁴, A. Kalweit³⁴, V. Kaplin⁹³, S. Kar⁶, A. Karasu Uysal⁷⁷, D. Karatovic⁹⁹, O. Karavichev⁶², T. Karavicheva⁶², P. Karczmarczyk¹⁴², E. Karpechev⁶², A. Kazantsev⁸⁸, U. Keschull⁷⁴, R. Keidel⁴⁷, M. Keil³⁴, B. Ketzer⁴³, Z. Khabanova⁹⁰, A.M. Khan⁶, S. Khan¹⁶, A. Khanzadeev⁹⁸, Y. Kharlov⁹¹, A. Khatun¹⁶, A. Khuntia¹¹⁸, B. Kileng³⁶, B. Kim⁶¹, B. Kim¹³³, D. Kim¹⁴⁷, D.J. Kim¹²⁶, E.J. Kim⁷³, H. Kim¹⁷, J. Kim¹⁴⁷, J.S. Kim⁴¹, J. Kim¹⁰⁴, J. Kim¹⁴⁷, J. Kim⁷³, M. Kim¹⁰⁴, S. Kim¹⁸, T. Kim¹⁴⁷, T. Kim¹⁴⁷, S. Kirsch⁶⁸, I. Kisel³⁹, S. Kiselev⁹², A. Kisiel¹⁴², J.L. Klay⁵, C. Klein⁶⁸, J. Klein^{34,59}, S. Klein⁸⁰, C. Klein-Bösing¹⁴⁴, M. Kleiner⁶⁸, A. Kluge³⁴, M.L. Knichel³⁴, A.G. Knospe¹²⁵, C. Kobdaj¹¹⁶, M.K. Köhler¹⁰⁴, T. Kollegger¹⁰⁷, A. Kondratyev⁷⁵, N. Kondratyeva⁹³, E. Kondratyuk⁹¹, J. König⁶⁸, S.A. Königstorfer¹⁰⁵, P.J. Konopka³⁴, G. Kornakov¹⁴², L. Koska¹¹⁷, O. Kovalenko⁸⁵, V. Kovalenko¹¹³, M. Kowalski¹¹⁸, I. Králik⁶⁴, A. Kravčáková³⁸, L. Kreis¹⁰⁷, M. Krivda^{64,111}, F. Krizek⁹⁵, K. Krizkova Gajdosova³⁷, M. Krüger⁶⁸, E. Kryshen⁹⁸, M. Krzewicki³⁹, A.M. Kubera⁹⁷, V. Kučera^{34,61}, C. Kuhn¹³⁶, P.G. Kuijjer⁹⁰, L. Kumar¹⁰⁰, S. Kundu⁸⁶, P. Kurashvili⁸⁵, A. Kurepin⁶², A.B. Kurepin⁶², A. Kuryakin¹⁰⁹, S. Kushpil⁹⁵, J. Kvapil¹¹¹, M.J. Kweon⁶¹, J.Y. Kwon⁶¹, Y. Kwon¹⁴⁷, S.L. La Pointe³⁹, P. La Rocca²⁷, Y.S. Lai⁸⁰, M. Lamanna³⁴, R. Langoy¹²⁹, K. Lapidus³⁴, A. Lardeux²⁰, P. Larionov⁵², E. Laudi³⁴, R. Lavicka³⁷, T. Lazareva¹¹³, R. Lea²⁴, L. Leardini¹⁰⁴, J. Lee¹³³, S. Lee¹⁴⁷, S. Lehner¹¹⁴, J. Lehrbach³⁹, R.C. Lemmon⁹⁴, I. León Monzón¹²⁰, E.D. Lesser¹⁹, M. Lettrich³⁴, P. Lévai¹⁴⁵, X. Li¹², X.L. Li⁶, J. Lien¹²⁹, R. Lietava¹¹¹, B. Lim¹⁷, V. Lindenstruth³⁹, A. Lindner⁴⁸, C. Lippmann¹⁰⁷, M.A. Lisa⁹⁷, A. Liu¹⁹, J. Liu¹²⁷, S. Liu⁹⁷, W.J. Llope¹⁴³, I.M. Lofnes²¹, V. Loginov⁹³, C. Loizides⁹⁶, P. Loncar³⁵, J.A. Lopez¹⁰⁴, X. Lopez¹³⁴, E. López Torres⁸, J.R. Luhder¹⁴⁴, M. Lunardon²⁸, G. Luparello⁶⁰, Y.G. Ma⁴⁰, A. Maevskaya⁶², M. Mager³⁴, S.M. Mahmood²⁰, T. Mahmoud⁴³, A. Maire¹³⁶, R.D. Majka^{146,i}, M. Malaev⁹⁸, Q.W. Malik²⁰, L. Malinina^{75,iv}, D. Mal'Kevich⁹², P. Malzacher¹⁰⁷, G. Mandaglio^{32,56}, V. Manko⁸⁸, F. Manso¹³⁴, V. Manzari⁵³, Y. Mao⁶, M. Marchisone¹³⁵, J. Mareš⁶⁶, G.V. Margagliotti²⁴, A. Margotti⁵⁴, A. Marín¹⁰⁷, C. Markert¹¹⁹, M. Marquard⁶⁸, C.D. Martin²⁴, N.A. Martin¹⁰⁴, P. Martinengo³⁴, J.L. Martinez¹²⁵, M.I. Martínez⁴⁵, G. Martínez García¹¹⁵, S. Masciocchi¹⁰⁷, M. Masera²⁵, A. Masoni⁵⁵, L. Massacrier⁷⁸, E. Masson¹¹⁵, A. Mastroserio^{53,138}, A.M. Mathis¹⁰⁵, O. Matonoha⁸¹, P.F.T. Matuoka¹²¹, A. Matyja¹¹⁸, C. Mayer¹¹⁸, F. Mazzaschi²⁵, M. Mazzilli⁵³, M.A. Mazzoni⁵⁸, A.F. Mechler⁶⁸, F. Meddi²², Y. Melikyan^{62,93}, A. Menchaca-Rocha⁷¹, E. Meninno^{29,114}, A.S. Menon¹²⁵, M. Meres¹³, S. Mhlanga¹²⁴, Y. Miake¹³³, L. Micheletti²⁵, L.C. Migliorin¹³⁵, D.L. Mihaylov¹⁰⁵, K. Mikhaylov^{75,92}, A.N. Mishra⁶⁹, D. Miśkowiec¹⁰⁷, A. Modak³, N. Mohammadi³⁴, A.P. Mohanty⁶³, B. Mohanty⁸⁶, M. Mohisin Khan^{16,v}, Z. Moravcova⁸⁹, C. Mordasini¹⁰⁵, D.A. Moreira De Godoy¹⁴⁴, L.A.P. Moreno⁴⁵, I. Morozov⁶², A. Morsch³⁴, T. Mrnjavac³⁴, V. Muccifora⁵², E. Mudnic³⁵, D. Mühlheim¹⁴⁴, S. Muhuri¹⁴¹, J.D. Mulligan⁸⁰, A. Mulliri^{23,55}, M.G. Munhoz¹²¹, R.H. Munzer⁶⁸, H. Murakami¹³², S. Murray¹²⁴, L. Musa³⁴, J. Musinsky⁶⁴, C.J. Myers¹²⁵, J.W. Myrcha¹⁴², B. Naik⁴⁹, R. Nair⁸⁵, B.K. Nandi⁴⁹, R. Nania^{10,54}, E. Nappi⁵³, M.U. Naru¹⁴, A.F. Nassirpour⁸¹, C. Nattrass¹³⁰, R. Nayak⁴⁹, T.K. Nayak⁸⁶, S. Nazarenko¹⁰⁹, A. Neagu²⁰, R.A. Negrao De Oliveira⁶⁸, L. Nellen⁶⁹, S.V. Nesbo³⁶, G. Neskovic³⁹, D. Nesterov¹¹³, L.T. Neumann¹⁴², B.S. Nielsen⁸⁹, S. Nikolaev⁸⁸, S. Nikulin⁸⁸, V. Nikulin⁹⁸, F. Noferini^{10,54}, P. Nomokonov⁷⁵, J. Norman^{79,127}, N. Novitzky¹³³, P. Nowakowski¹⁴², A. Nyanin⁸⁸, J. Nystrand²¹, M. Ogino⁸², A. Ohlson^{81,104}, J. Olińczak¹⁴², A.C. Oliveira Da Silva¹³⁰, M.H. Oliver¹⁴⁶, C. Oppedisano⁵⁹, A. Ortiz Velasquez⁶⁹, A. Oskarsson⁸¹, J. Otwinowski¹¹⁸, K. Oyama⁸², Y. Pachmayer¹⁰⁴, V. Pacik⁸⁹, S. Padhan⁴⁹, D. Pagano¹⁴⁰, G. Paic⁶⁹, J. Pan¹⁴³, S. Panebianco¹³⁷, P. Pareek^{50,141}, J. Park⁶¹, J.E. Parkkila¹²⁶, S. Parmar¹⁰⁰, S.P. Pathak¹²⁵, B. Paul²³, J. Pazzini¹⁴⁰, H. Pei⁶, T. Peitzmann⁶³, X. Peng⁶, L.G. Pereira⁷⁰, H. Pereira Da Costa¹³⁷, D. Peresunko⁸⁸, G.M. Perez⁸, S. Perrin¹³⁷, Y. Pestov⁴, V. Petráček³⁷, M. Petrovici⁴⁸, R.P. Pezzi⁷⁰, S. Piano⁶⁰, M. Pikna¹³, P. Pillot¹¹⁵, O. Pinazza^{34,54}, L. Pinsky¹²⁵, C. Pinto²⁷, S. Pisano^{10,52}, D. Pistone⁵⁶, M. Płoskoń⁸⁰, M. Planinic⁹⁹, F. Pliquett⁶⁸, M.G. Poghosyan⁹⁶, B. Polichtchouk⁹¹, N. Poljak⁹⁹, A. Pop⁴⁸, S. Porteboeuf-Houssais¹³⁴, V. Pozdniakov⁷⁵, S.K. Prasad³, R. Preghenella⁵⁴, F. Prino⁵⁹, C.A. Pruneau¹⁴³, I. Pshenichnov⁶², M. Puccio³⁴, J. Putschke¹⁴³, S. Qiu⁹⁰, L. Quaglia²⁵, R.E. Quishpe¹²⁵, S. Ragoni¹¹¹, S. Raha³, S. Rajput¹⁰¹, J. Rak¹²⁶, A. Rakotozafindrabe¹³⁷, L. Ramello³¹, F. Rami¹³⁶, S.A.R. Ramirez⁴⁵, R. Raniwala¹⁰², S. Raniwala¹⁰², S.S. Räsänen⁴⁴, R. Rath⁵⁰, V. Ratza⁴³, I. Ravasenga⁹⁰, K.F. Read^{96,130}, A.R. Redelbach³⁹, K. Redlich^{85,vi}, A. Rehman²¹, P. Reichelt⁶⁸, F. Reidt³⁴, X. Ren⁶, R. Renfordt⁶⁸, Z. Rescakova³⁸, K. Reygers¹⁰⁴, A. Riabov⁹⁸, V. Riabov⁹⁸, T. Richert^{81,89}, M. Richter²⁰, P. Riedler³⁴, W. Riegler³⁴, F. Riggi²⁷, C. Ristea⁶⁷, S.P. Rode⁵⁰,

M. Rodríguez Cahuantzi⁴⁵, K. Røed²⁰, R. Rogalev⁹¹, E. Rogochaya⁷⁵, D. Rohr³⁴, D. Röhrich²¹, P.F. Rojas⁴⁵, P.S. Rokita¹⁴², F. Ronchetti⁵², A. Rosano⁵⁶, E.D. Rosas⁶⁹, K. Roslon¹⁴², P. Rosnet¹³⁴, A. Rossi^{28,57}, A. Rotondi¹³⁹, A. Roy⁵⁰, P. Roy¹¹⁰, O.V. Rueda⁸¹, R. Rui²⁴, B. Rumyantsev⁷⁵, A. Rustamov⁸⁷, E. Ryabinkin⁸⁸, Y. Ryabov⁹⁸, A. Rybicki¹¹⁸, H. Rytkonen¹²⁶, O.A.M. Saarimaki⁴⁴, R. Sadek¹¹⁵, S. Sadhu¹⁴¹, S. Sadovsky⁹¹, K. Šafařík³⁷, S.K. Saha¹⁴¹, B. Sahoo⁴⁹, P. Sahoo⁴⁹, R. Sahoo⁵⁰, S. Sahoo⁶⁵, P.K. Sahu⁶⁵, J. Saini¹⁴¹, S. Sakai¹³³, S. Sambyal¹⁰¹, V. Samsonov^{93,98}, D. Sarkar¹⁴³, N. Sarkar¹⁴¹, P. Sarma⁴², V.M. Sarti¹⁰⁵, M.H.P. Sas⁶³, E. Scapparone⁵⁴, J. Schambach¹¹⁹, H.S. Scheid⁶⁸, C. Schiaua⁴⁸, R. Schicker¹⁰⁴, A. Schmah¹⁰⁴, C. Schmidt¹⁰⁷, H.R. Schmidt¹⁰³, M.O. Schmidt¹⁰⁴, M. Schmidt¹⁰³, N.V. Schmidt^{68,96}, A.R. Schmier¹³⁰, J. Schukraft⁸⁹, Y. Schutz¹³⁶, K. Schwarz¹⁰⁷, K. Schweda¹⁰⁷, G. Scioli²⁶, E. Scomparin⁵⁹, J.E. Seger¹⁵, Y. Sekiguchi¹³², D. Sekihata¹³², I. Selyuzhenkov^{93,107}, S. Senyukov¹³⁶, D. Serebryakov⁶², A. Sevcenco⁶⁷, A. Shabanov⁶², A. Shabetai¹¹⁵, R. Shahoyan³⁴, W. Shaikh¹¹⁰, A. Shangaraev⁹¹, A. Sharma¹⁰⁰, A. Sharma¹⁰¹, H. Sharma¹¹⁸, M. Sharma¹⁰¹, N. Sharma¹⁰⁰, S. Sharma¹⁰¹, O. Sheibani¹²⁵, K. Shigaki⁴⁶, M. Shimomura⁸³, S. Shirinkin⁹², Q. Shou⁴⁰, Y. Sibiriak⁸⁸, S. Siddhanta⁵⁵, T. Siemiarzuk⁸⁵, D. Silvermyr⁸¹, G. Simatovic⁹⁰, G. Simonetti³⁴, B. Singh¹⁰⁵, R. Singh⁸⁶, R. Singh¹⁰¹, R. Singh⁵⁰, V.K. Singh¹⁴¹, V. Singhal¹⁴¹, T. Sinha¹¹⁰, B. Sitar¹³, M. Sitta³¹, T.B. Skaali²⁰, M. Slupecki⁴⁴, N. Smirnov¹⁴⁶, R.J.M. Snellings⁶³, C. Soncco¹¹², J. Song¹²⁵, A. Songmoolnak¹¹⁶, F. Soramel²⁸, S. Sorensen¹³⁰, I. Sputowska¹¹⁸, J. Stachel¹⁰⁴, I. Stan⁶⁷, P.J. Steffanic¹³⁰, E. Stenlund⁸¹, S.F. Stiefelmaier¹⁰⁴, D. Stocco¹¹⁵, M.M. Storetvedt³⁶, L.D. Stritto²⁹, A.A.P. Suaide¹²¹, T. Sugitate⁴⁶, C. Suire⁷⁸, M. Suleymanov¹⁴, M. Suljic³⁴, R. Sultanov⁹², M. Šumbera⁹⁵, V. Sumberia¹⁰¹, S. Sumowidagdo⁵¹, S. Swain⁶⁵, A. Szabo¹³, I. Szarka¹³, U. Tabassam¹⁴, S.F. Taghavi¹⁰⁵, G. Taillepie¹³⁴, J. Takahashi¹²², G.J. Tambave²¹, S. Tang^{6,134}, M. Tarhini¹¹⁵, M.G. Tarzila⁴⁸, A. Tauro³⁴, G. Tejada Muñoz⁴⁵, A. Telesca³⁴, L. Terlizzi²⁵, C. Terrevoli¹²⁵, D. Thakur⁵⁰, S. Thakur¹⁴¹, D. Thomas¹¹⁹, F. Thoresen⁸⁹, R. Tieulent¹³⁵, A. Tikhonov⁶², A.R. Timmins¹²⁵, A. Toia⁶⁸, N. Topilskaya⁶², M. Toppi⁵², F. Torales-Acosta¹⁹, S.R. Torres³⁷, A. Trifiro^{32,56}, S. Tripathy^{50,69}, T. Tripathy⁴⁹, S. Trogolo²⁸, G. Trombetta³³, L. Tropp³⁸, V. Trubnikov², W.H. Trzaska¹²⁶, T.P. Trzcinski¹⁴², B.A. Trzeciak^{37,63}, A. Tumkin¹⁰⁹, R. Turrisi⁵⁷, T.S. Tveter²⁰, K. Ullaland²¹, E.N. Umaka¹²⁵, A. Uras¹³⁵, G.L. Usai²³, M. Vala³⁸, N. Valle¹³⁹, S. Vallero⁵⁹, N. van der Kolk⁶³, L.V.R. van Doremalen⁶³, M. van Leeuwen⁶³, P. Vande Vyvre³⁴, D. Varga¹⁴⁵, Z. Varga¹⁴⁵, M. Varga-Kofarago¹⁴⁵, A. Vargas⁴⁵, M. Vasileiou⁸⁴, A. Vasiliev⁸⁸, O. Vázquez Doce¹⁰⁵, V. Vechernin¹¹³, E. Vercellin²⁵, S. Vergara Limón⁴⁵, L. Vermunt⁶³, R. Vernet⁷, R. Vértesi¹⁴⁵, L. Vickovic³⁵, Z. Vilakazi¹³¹, O. Villalobos Baillie¹¹¹, G. Vino⁵³, A. Vinogradov⁸⁸, T. Virgili²⁹, V. Vislavicius⁸⁹, A. Vodopyanov⁷⁵, B. Volkel³⁴, M.A. Völkl¹⁰³, K. Voloshin⁹², S.A. Voloshin¹⁴³, G. Volpe³³, B. von Haller³⁴, I. Vorobyev¹⁰⁵, D. Voscek¹¹⁷, J. Vrláková³⁸, B. Wagner²¹, M. Weber¹¹⁴, S.G. Weber¹⁴⁴, A. Wegrzynek³⁴, S.C. Wenzel³⁴, J.P. Wessels¹⁴⁴, J. Wiechula⁶⁸, J. Wikne²⁰, G. Wilk⁸⁵, J. Wilkinson^{10,54}, G.A. Willems¹⁴⁴, E. Willsher¹¹¹, B. Windelband¹⁰⁴, M. Winn¹³⁷, W.E. Witt¹³⁰, J.R. Wright¹¹⁹, Y. Wu¹²⁸, R. Xu⁶, S. Yalcin⁷⁷, Y. Yamaguchi⁴⁶, K. Yamakawa⁴⁶, S. Yang²¹, S. Yano¹³⁷, Z. Yin⁶, H. Yokoyama⁶³, I.-K. Yoo¹⁷, J.H. Yoon⁶¹, S. Yuan²¹, A. Yuncu¹⁰⁴, V. Yurchenko², V. Zaccolo²⁴, A. Zaman¹⁴, C. Zampolli³⁴, H.J.C. Zanolli⁶³, N. Zardoshti³⁴, A. Zarochentsev¹¹³, P. Závada⁶⁶, N. Zaviyalov¹⁰⁹, H. Zbroszczyk¹⁴², M. Zhalov⁹⁸, S. Zhang⁴⁰, X. Zhang⁶, Z. Zhang⁶, V. Zhrebchevskii¹¹³, Y. Zhi¹², D. Zhou⁶, Y. Zhou⁸⁹, Z. Zhou²¹, J. Zhu^{6,107}, Y. Zhu⁶, A. Zichichi^{10,26}, G. Zinovjev², N. Zurlo¹⁴⁰,

Affiliation notes

- ⁱ Deceased
- ⁱⁱ Italian National Agency for New Technologies, Energy and Sustainable Economic Development (ENEA), Bologna, Italy
- ⁱⁱⁱ Dipartimento DET del Politecnico di Torino, Turin, Italy
- ^{iv} M.V. Lomonosov Moscow State University, D.V. Skobeltsyn Institute of Nuclear Physics, Moscow, Russia
- ^v Department of Applied Physics, Aligarh Muslim University, Aligarh, India
- ^{vi} Institute of Theoretical Physics, University of Wrocław, Poland

Collaboration Institutes

- ¹ A.I. Alikhanyan National Science Laboratory (Yerevan Physics Institute) Foundation, Yerevan, Armenia
- ² Bogolyubov Institute for Theoretical Physics, National Academy of Sciences of Ukraine, Kiev, Ukraine
- ³ Bose Institute, Department of Physics and Centre for Astroparticle Physics and Space Science (CAPSS), Kolkata, India
- ⁴ Budker Institute for Nuclear Physics, Novosibirsk, Russia
- ⁵ California Polytechnic State University, San Luis Obispo, California, United States

- 6 Central China Normal University, Wuhan, China
- 7 Centre de Calcul de l'IN2P3, Villeurbanne, Lyon, France
- 8 Centro de Aplicaciones Tecnológicas y Desarrollo Nuclear (CEADEN), Havana, Cuba
- 9 Centro de Investigación y de Estudios Avanzados (CINVESTAV), Mexico City and Mérida, Mexico
- 10 Centro Fermi - Museo Storico della Fisica e Centro Studi e Ricerche "Enrico Fermi", Rome, Italy
- 11 Chicago State University, Chicago, Illinois, United States
- 12 China Institute of Atomic Energy, Beijing, China
- 13 Comenius University Bratislava, Faculty of Mathematics, Physics and Informatics, Bratislava, Slovakia
- 14 COMSATS University Islamabad, Islamabad, Pakistan
- 15 Creighton University, Omaha, Nebraska, United States
- 16 Department of Physics, Aligarh Muslim University, Aligarh, India
- 17 Department of Physics, Pusan National University, Pusan, Republic of Korea
- 18 Department of Physics, Sejong University, Seoul, Republic of Korea
- 19 Department of Physics, University of California, Berkeley, California, United States
- 20 Department of Physics, University of Oslo, Oslo, Norway
- 21 Department of Physics and Technology, University of Bergen, Bergen, Norway
- 22 Dipartimento di Fisica dell'Università 'La Sapienza' and Sezione INFN, Rome, Italy
- 23 Dipartimento di Fisica dell'Università and Sezione INFN, Cagliari, Italy
- 24 Dipartimento di Fisica dell'Università and Sezione INFN, Trieste, Italy
- 25 Dipartimento di Fisica dell'Università and Sezione INFN, Turin, Italy
- 26 Dipartimento di Fisica e Astronomia dell'Università and Sezione INFN, Bologna, Italy
- 27 Dipartimento di Fisica e Astronomia dell'Università and Sezione INFN, Catania, Italy
- 28 Dipartimento di Fisica e Astronomia dell'Università and Sezione INFN, Padova, Italy
- 29 Dipartimento di Fisica 'E.R. Caianiello' dell'Università and Gruppo Collegato INFN, Salerno, Italy
- 30 Dipartimento DISAT del Politecnico and Sezione INFN, Turin, Italy
- 31 Dipartimento di Scienze e Innovazione Tecnologica dell'Università del Piemonte Orientale and INFN Sezione di Torino, Alessandria, Italy
- 32 Dipartimento di Scienze MIFT, Università di Messina, Messina, Italy
- 33 Dipartimento Interateneo di Fisica 'M. Merlin' and Sezione INFN, Bari, Italy
- 34 European Organization for Nuclear Research (CERN), Geneva, Switzerland
- 35 Faculty of Electrical Engineering, Mechanical Engineering and Naval Architecture, University of Split, Split, Croatia
- 36 Faculty of Engineering and Science, Western Norway University of Applied Sciences, Bergen, Norway
- 37 Faculty of Nuclear Sciences and Physical Engineering, Czech Technical University in Prague, Prague, Czech Republic
- 38 Faculty of Science, P.J. Šafárik University, Košice, Slovakia
- 39 Frankfurt Institute for Advanced Studies, Johann Wolfgang Goethe-Universität Frankfurt, Frankfurt, Germany
- 40 Fudan University, Shanghai, China
- 41 Gangneung-Wonju National University, Gangneung, Republic of Korea
- 42 Gauhati University, Department of Physics, Guwahati, India
- 43 Helmholtz-Institut für Strahlen- und Kernphysik, Rheinische Friedrich-Wilhelms-Universität Bonn, Bonn, Germany
- 44 Helsinki Institute of Physics (HIP), Helsinki, Finland
- 45 High Energy Physics Group, Universidad Autónoma de Puebla, Puebla, Mexico
- 46 Hiroshima University, Hiroshima, Japan
- 47 Hochschule Worms, Zentrum für Technologietransfer und Telekommunikation (ZTT), Worms, Germany
- 48 Horia Hulubei National Institute of Physics and Nuclear Engineering, Bucharest, Romania
- 49 Indian Institute of Technology Bombay (IIT), Mumbai, India
- 50 Indian Institute of Technology Indore, Indore, India
- 51 Indonesian Institute of Sciences, Jakarta, Indonesia
- 52 INFN, Laboratori Nazionali di Frascati, Frascati, Italy
- 53 INFN, Sezione di Bari, Bari, Italy
- 54 INFN, Sezione di Bologna, Bologna, Italy
- 55 INFN, Sezione di Cagliari, Cagliari, Italy
- 56 INFN, Sezione di Catania, Catania, Italy

- 57 INFN, Sezione di Padova, Padova, Italy
- 58 INFN, Sezione di Roma, Rome, Italy
- 59 INFN, Sezione di Torino, Turin, Italy
- 60 INFN, Sezione di Trieste, Trieste, Italy
- 61 Inha University, Incheon, Republic of Korea
- 62 Institute for Nuclear Research, Academy of Sciences, Moscow, Russia
- 63 Institute for Subatomic Physics, Utrecht University/Nikhef, Utrecht, Netherlands
- 64 Institute of Experimental Physics, Slovak Academy of Sciences, Košice, Slovakia
- 65 Institute of Physics, Homi Bhabha National Institute, Bhubaneswar, India
- 66 Institute of Physics of the Czech Academy of Sciences, Prague, Czech Republic
- 67 Institute of Space Science (ISS), Bucharest, Romania
- 68 Institut für Kernphysik, Johann Wolfgang Goethe-Universität Frankfurt, Frankfurt, Germany
- 69 Instituto de Ciencias Nucleares, Universidad Nacional Autónoma de México, Mexico City, Mexico
- 70 Instituto de Física, Universidade Federal do Rio Grande do Sul (UFRGS), Porto Alegre, Brazil
- 71 Instituto de Física, Universidad Nacional Autónoma de México, Mexico City, Mexico
- 72 iThemba LABS, National Research Foundation, Somerset West, South Africa
- 73 Jeonbuk National University, Jeonju, Republic of Korea
- 74 Johann-Wolfgang-Goethe Universität Frankfurt Institut für Informatik, Fachbereich Informatik und Mathematik, Frankfurt, Germany
- 75 Joint Institute for Nuclear Research (JINR), Dubna, Russia
- 76 Korea Institute of Science and Technology Information, Daejeon, Republic of Korea
- 77 KTO Karatay University, Konya, Turkey
- 78 Laboratoire de Physique des 2 Infinis, Irène Joliot-Curie, Orsay, France
- 79 Laboratoire de Physique Subatomique et de Cosmologie, Université Grenoble-Alpes, CNRS-IN2P3, Grenoble, France
- 80 Lawrence Berkeley National Laboratory, Berkeley, California, United States
- 81 Lund University Department of Physics, Division of Particle Physics, Lund, Sweden
- 82 Nagasaki Institute of Applied Science, Nagasaki, Japan
- 83 Nara Women's University (NWU), Nara, Japan
- 84 National and Kapodistrian University of Athens, School of Science, Department of Physics, Athens, Greece
- 85 National Centre for Nuclear Research, Warsaw, Poland
- 86 National Institute of Science Education and Research, Homi Bhabha National Institute, Jatni, India
- 87 National Nuclear Research Center, Baku, Azerbaijan
- 88 National Research Centre Kurchatov Institute, Moscow, Russia
- 89 Niels Bohr Institute, University of Copenhagen, Copenhagen, Denmark
- 90 Nikhef, National institute for subatomic physics, Amsterdam, Netherlands
- 91 NRC Kurchatov Institute IHEP, Protvino, Russia
- 92 NRC «Kurchatov» Institute - ITEP, Moscow, Russia
- 93 NRNU Moscow Engineering Physics Institute, Moscow, Russia
- 94 Nuclear Physics Group, STFC Daresbury Laboratory, Daresbury, United Kingdom
- 95 Nuclear Physics Institute of the Czech Academy of Sciences, Řež u Prahy, Czech Republic
- 96 Oak Ridge National Laboratory, Oak Ridge, Tennessee, United States
- 97 Ohio State University, Columbus, Ohio, United States
- 98 Petersburg Nuclear Physics Institute, Gatchina, Russia
- 99 Physics department, Faculty of science, University of Zagreb, Zagreb, Croatia
- 100 Physics Department, Panjab University, Chandigarh, India
- 101 Physics Department, University of Jammu, Jammu, India
- 102 Physics Department, University of Rajasthan, Jaipur, India
- 103 Physikalisches Institut, Eberhard-Karls-Universität Tübingen, Tübingen, Germany
- 104 Physikalisches Institut, Ruprecht-Karls-Universität Heidelberg, Heidelberg, Germany
- 105 Physik Department, Technische Universität München, Munich, Germany
- 106 Politecnico di Bari, Bari, Italy
- 107 Research Division and ExtreMe Matter Institute EMMI, GSI Helmholtzzentrum für Schwerionenforschung GmbH, Darmstadt, Germany
- 108 Rudjer Bošković Institute, Zagreb, Croatia

- 109 Russian Federal Nuclear Center (VNIIEF), Sarov, Russia
- 110 Saha Institute of Nuclear Physics, Homi Bhabha National Institute, Kolkata, India
- 111 School of Physics and Astronomy, University of Birmingham, Birmingham, United Kingdom
- 112 Sección Física, Departamento de Ciencias, Pontificia Universidad Católica del Perú, Lima, Peru
- 113 St. Petersburg State University, St. Petersburg, Russia
- 114 Stefan Meyer Institut für Subatomare Physik (SMI), Vienna, Austria
- 115 SUBATECH, IMT Atlantique, Université de Nantes, CNRS-IN2P3, Nantes, France
- 116 Suranaree University of Technology, Nakhon Ratchasima, Thailand
- 117 Technical University of Košice, Košice, Slovakia
- 118 The Henryk Niewodniczanski Institute of Nuclear Physics, Polish Academy of Sciences, Cracow, Poland
- 119 The University of Texas at Austin, Austin, Texas, United States
- 120 Universidad Autónoma de Sinaloa, Culiacán, Mexico
- 121 Universidade de São Paulo (USP), São Paulo, Brazil
- 122 Universidade Estadual de Campinas (UNICAMP), Campinas, Brazil
- 123 Universidade Federal do ABC, Santo Andre, Brazil
- 124 University of Cape Town, Cape Town, South Africa
- 125 University of Houston, Houston, Texas, United States
- 126 University of Jyväskylä, Jyväskylä, Finland
- 127 University of Liverpool, Liverpool, United Kingdom
- 128 University of Science and Technology of China, Hefei, China
- 129 University of South-Eastern Norway, Tonsberg, Norway
- 130 University of Tennessee, Knoxville, Tennessee, United States
- 131 University of the Witwatersrand, Johannesburg, South Africa
- 132 University of Tokyo, Tokyo, Japan
- 133 University of Tsukuba, Tsukuba, Japan
- 134 Université Clermont Auvergne, CNRS/IN2P3, LPC, Clermont-Ferrand, France
- 135 Université de Lyon, Université Lyon 1, CNRS/IN2P3, IPN-Lyon, Villeurbanne, Lyon, France
- 136 Université de Strasbourg, CNRS, IPHC UMR 7178, F-67000 Strasbourg, France, Strasbourg, France
- 137 Université Paris-Saclay Centre d'Etudes de Saclay (CEA), IRFU, Département de Physique Nucléaire (DPhN), Saclay, France
- 138 Università degli Studi di Foggia, Foggia, Italy
- 139 Università degli Studi di Pavia, Pavia, Italy
- 140 Università di Brescia, Brescia, Italy
- 141 Variable Energy Cyclotron Centre, Homi Bhabha National Institute, Kolkata, India
- 142 Warsaw University of Technology, Warsaw, Poland
- 143 Wayne State University, Detroit, Michigan, United States
- 144 Westfälische Wilhelms-Universität Münster, Institut für Kernphysik, Münster, Germany
- 145 Wigner Research Centre for Physics, Budapest, Hungary
- 146 Yale University, New Haven, Connecticut, United States
- 147 Yonsei University, Seoul, Republic of Korea